Synthesis, Characterization, Cytotoxic Studies of $[(\eta^5\text{-}C_5H_5)_2Mo(\text{thionucleobase/thionucleoside})]Cl$ Complexes on Cancer Cell Lines and their Interaction with Human Serum Albumin

By
Débora Acevedo-Acevedo

A thesis submitted in partial fulfillment of the requirements for the degree of

Master in Science
in
Chemistry

University of Puerto Rico
Mayagüez Campus
2010

Approved by:

_____	_____
José E. Cortés-Figueroa, PhD Member, Graduate Committee	Date
_____	_____
Gustavo López, PhD Member, Graduate Committee	Date
_____	_____
Enrique Meléndez-Martínez, PhD President, Graduate Committee	Date
_____	_____
Jayanta Banejee, PhD Representative of Graduate Studies	Date
_____	_____
Francis Patrón, PhD Chairperson of Chemistry Department	Date

Abstract

Molybdenocene dichloride like some other metallocene dihalides Cp_2MX_2 (M = Ti, V, Nb, Mo and X = halides) have shown high antiproliferative properties against a wide range of murine and human tumors. They also exhibit less toxic side effects than platinum antitumor agents. In this work we present the synthesis of four complexes of molybdenocene at physiological pH in aqueous medium. The complexes $[(\eta^5\text{-}C_5H_5)_2Mo(L)]Cl$ (L=6-mercaptopurine , 6-mercaptopurine ribose, (-)-2-amino-6-mercaptopurine and (-)-2-amino-6-mercaptopurine ribose) were characterized by FT-IR, NMR, MS and elemental analysis.

The synthesized, characterized and purified complexes were interacted with Human Serum Albumin (HSA), a 66.5 kDa protein with an impressive array of binding sites capable of binding a wide variety of ligands. The interaction between HSA with Cp_2MoCl_2 and $[Cp_2Mo(L)]Cl$ complexes was monitored by UV-Vis from 200 – 600 nm observing no new bands or isosbestic point and by NMR at 25 and 37ºC. Such interactions were not observed unlike to what was hypothesized by Harding et al.

Cytotoxic studies were also performed on the four new molybdenocene derivatives on HT-29 colon cancer and MCF-7 breast cancer cell lines. These studies were compared to those carried out for molybdenocene dichloride. Complexes that contained ribose showed to be less active than those without ribose but all complexes proved to have more cytotoxic activity than molybdenocene dichloride in HT-29 colon cancer. In MCF-7 breast cancer, the addition of these bidentate ligands without a ribose group, improves the cytotoxic activity when compared to Cp_2MoCl_2. On the other hand the complexes with the ribose groups showed to be not active in MCF-7 cell line.

Resumen

Dicloruro de molibdenoceno al igual que otros dihaluros de metalocenos Cp_2MX_2 (M = Ti, V, Nb, Mo and X = haluros) han demostrado propiedades antiproliferativas en contra de una amplia gama de tumores humanos y de ratas. También han demostrado menos efectos tóxicos secundarios en comparación con agentes antitumorales de platino. En éste trabajo presentamos la síntesis de cuatro complejos de molibdenoceno en un medio acuoso con pH fisiológico. Los complejos $[(\eta^5\text{-}C_5H_5)_2Mo(L)]Cl$ (L=6-mercaptopurina , 6-mercaptopurina ribosa , (-)-2-amino-6-mercaptopurina y (-)-2-amino-6-mercaptopurina ribosa) fueron caracterizados por infrarrojo con transformada de Fourier (FT-IR, por sus siglas en inglés), Resonancia Magnética Nuclear (NMR, por sus siglas en inglés), Espectrometría de Masas (MS, por sus siglas en inglés) y Análisis Elemental.

Los complejos sintetizados caracterizados y purificados fueron interactuados con Albúmina de Suero Humano (HSA, por sus siglas en inglés), una proteína de 66.5 kDa con una gama impresionante de sitios de enlazamiento la cual es capaz de enlazar una gran variedad de ligandos. La interacción entre HAS con los complejos Cp_2MoCl_2 y $[Cp_2Mo(L)]Cl$ fue monitoreada utilizando espectroscopía ultravioleta visible (UV-Vis) en la región de 200 – 600 nm, donde no se observaron ningunas bandas nuevas o puntos isosbésticos como tampoco se observaron cambios en desplazamientos químicos en NMR a 25 y 37 ºC. Dichas interacciones no se observaron al contrario de lo que fue reportado por Harding et al.

Estudios citotóxicos también se llevaron a cabo utilizando los cuatro complejos nuevos de derivados de molibdenoceno en la línea celular HT-29 del cáncer del colon y la línea celular MCF-7 del cáncer del ceno. Estos estudios se compararon con aquellos llevados a cabo con dicloruro de molibdenoceno. Los complejos que contenían ribosa demostraron ser menos

activos en comparación con los que no contenían ribosa, pero todos los complejos probaron tener más actividad que dicloruro de molibdenoceno en la actividad citotóxica hacia la línea celular HT-29 del cáncer del colon. En la línea celular MCF-7 del cáncer del seno la adición de éstos ligandos bidentados sin el grupo ribosa mejoró la actividad citotóxica en comparación con Cp_2MoCl_2. Por el contrario los complejos con el grupo ribosa no demostraron tener actividad en la línea MCF-7.

to Evan Arthur Hagman-Acevedo and Elvin Igartúa-Nieves

Acknowledgements

I would like to thank Dr. Enrique Meléndez, Dr. Li Ming Gao, José L. Vera, Idainés Feliciano, José Lamboy and Aracelys Cardona for their training and experimental assistance. I would also like to thank Elvin Igartúa, Cacimar Ramos, Madeline S. León and Laura B. Granell for their support.

NIH MBRS SCORE Programs at both the University of Puerto Rico Mayaguez and the Ponce School of Medicine for financial support via NIH-MBRS-SCORE Program grant #S06 GM008239-23 and the PSM-Moffitt Cancer Center Partnership 1U56CA126379-01. Bridge to The Doctorate Program, Science on Wheels and GLOBE Programs and the Alliance for Minority Participation for their financial support.

Finally Dr. Jaime Matta and his group for their training and experimental assistance in cyotoxic studies at the Ponce School of Medicine are greatly acknowledged.

Table of Contents

Table List

Table **Page**

Figure List

Figure **Page**

1. Introduction

Over the years heart disease took one of the top places in mortality, however it is expected that cancer will become the leading cause of death worldwide during 2010, according to World Health Organization. Cancer is one of the leading diseases that cause death in the world. In a natural process, cells are produced and divided according to the needs of the human body. Once they age, they self-destroy due to a process known as apoptosis, and at the same time newer cells are created. There is a possibility that some cells may lose their ability to maintain this balance (division and apoptosis), as a consequence they start to grow uncontrollably. They lose the ability to destroy themselves, thus forming a mass of tissue known as tumor or neoplasm. There are two kinds of tumors, the benign or malignant. The later may attack other organs and tissues by traveling through the bloodstream in a process called metastasis, or simply invade nearby tissues. It is the malignant tumor that is known as cancer.

There are over 100 types of cancer were scientists have classified the neoplasm as their origin [1]. Carcinomas are those neoplasms that originate from epithelial cells. Sarcomas originate in the bones, muscles and connective tissues of the body. Lymphomas originate in the tissues of the body's immune system and leukemia is cancer that originates in the bone marrow and accumulates in the bloodstream.

Cancer strikes people regardless of age, sex or national origin. Although scientists cannot attribute the cancer to a single reason, exposure to radiation, an unbalanced diet, genetics, hormonal disorders, some chemicals and pollution are some factors identified as potential causes of cancer.

There are currently several treatments for cancer including surgery, radiotherapy and chemotherapy. Transition metals have also been incorporated into cancer treatments. In the year 1978 the FDA approved the first drug based on platinum *cis*-$PtCl_2(NH_3)_2$, better known as cis-platin [2]. Cis-platin is an antineoplastic drug that prevents the development of cancerous cells. It was the first of platinum complex that were used as anti-neoplastic drugs, others include: carboplatin, oxaliplatin and nedaplatin (Figure 1). These platinum complexes bind to cellular DNA. If the DNA lesion is not repaired by the cell, then cell death can occur avoiding the proliferation of cancer cells.

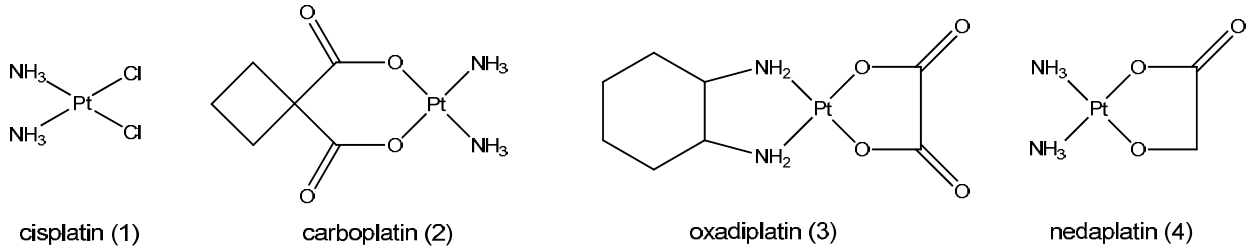

Figure 1 Molecular structure of anti-neoplastic drugs based on platinum.

Although it is good to know there are treatments for cancer, we cannot ignore the side effects that in some way or another affect the quality of life of patients with this disease. Some of the side effects of these treatments include hair loss, nausea, incontinence, change in behavior, and thyroid problems among others [3-6]. It has also been found that these drugs and treatments can kill both normal cells and cancer cells. It is for this reason that scientists cannot stop the effort to find treatments that are effective, selective and not ruined the quality of life of people suffering some form of cancer.

By the late 70's early 80's scientists Petra Köpf-Maier and Dr. Hartmut Köpf detected antitumor activity in compounds with transition metals. [7-9]. This discovery opened to a new area of study, metallocenes.

Metallocenes such as Cp_2MCl_2 (M = Ti, V, Ni and Mo, Cp = $C_5H_5^-$) (Figure 2) have shown to possess antitumor activity in colon, lung and breast cancer [9-15]. Some studies have also shown that these compounds are less toxic than cis-platin. A disadvantage in metallocenes is that they possess little hydrolytic stability in aqueous solutions, particularly at physiological pH, and show little solubility in water [16-17]. Of all the metallocenes studied today, titanocene is the only metallocene that is currently in phase II clinical trials.

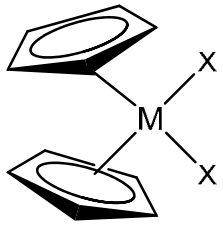

Figure 2 Basic structure of metallocenes

Metallocenes such as vanadocene, titanocene and molydenocene dichlorides have shown to be species with antitumor properties. In 2004 Vinclarek et al. studied the interaction of vanadocene with phosphate buffered saline in order to deliberate the stability of the new vanadocene complex and also to study its behavior in aqueous solution. It was found that stability of vanadocene fragment increases as a consequence of the interaction as a 4-member chelate bonded phosphate ligand and for that reason the vanadocene fragment is more resistant toward to degradation at physiologic pH. Now the chelate cycle is sufficiently labile to be replaced by another ligands during hydrolytic reaction. As a result, cis-positions of vanadocene

fragment are available for reactions with biomolecules such as proteins, which is essential for antitumor effect of vanadocene complexes. [18]

The interactions of some vanadocene and other metallocenes complexes with sulfur containing amino acids have been studied at a molecular level in order to understand their antiproliferative activity [19-21]. It has been found that the amino acid derivatives are air-stable and highly water-soluble, making them promising candidates for clinical studies. Besides studying the physical and chemical properties of metallocene derivatives it is important to study the transport of the metallocene to the target places in cancer cells. This is an important aspect to obtain mechanistic information and the study of the interaction of metallocene with certain proteins, thus resolving the metal-to-cell transporting potential of the protein. It has been proposed that transferrin and albumin (Figure 3) to be possible medium of transports of the metal trough the blood stream.

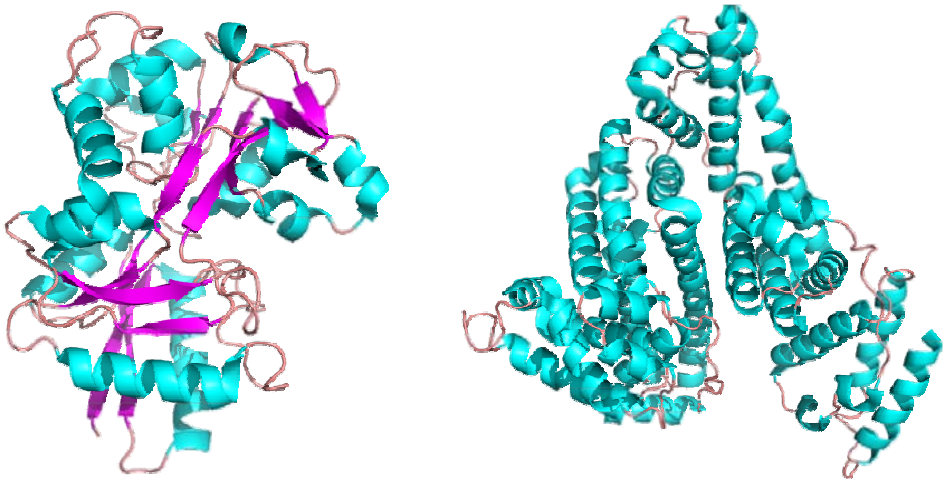

Transferrin pdb:1d4n (1) Human serum albumin pdb:1E78 (2)

Figure 3 Transferrin and Human Serum Albumin metal carrier proteins structures.

Transferrin is a glycoprotein with a molecular mass of approximately 80kD. It has two lobes that are known as N and C; it is in these lobes where the active site of binding metals takes place. Two tyrosine residues, one aspartate residue, one histidine residue and a synergetic anion conform the metal binding sites (Figure 4) [22-23]. The main function of both lobes is to transport iron(III) through the blood. Studies have shown that human transferrin has the ability to bind other metal ions at iron-specific binding sites and acts as a delivery system of metals into the cells [25]. Studies have shown that metals such as titanium and vanadium bind to tranferrin and also this protein is responsible for the transport of titanium complexes to tumor cells. [24,26,38]

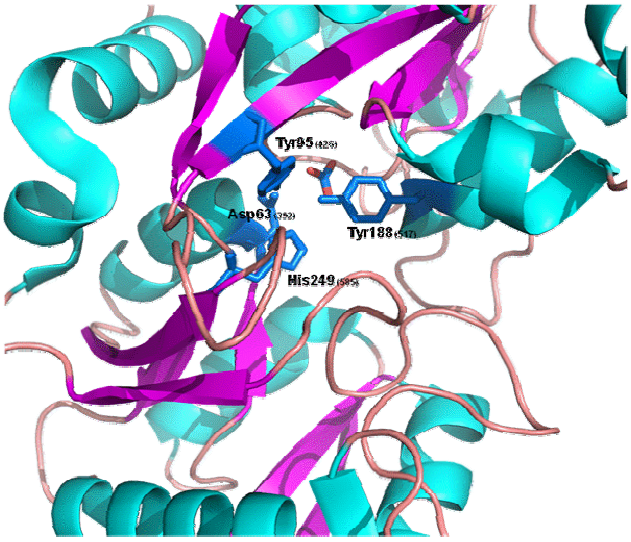

Figure 4 Tranferrin metal binding site structure.

Human serum albumin (HSA), a 66.5 kDa globular protein, is the most abundant protein in the blood plasma and is capable of binding ion metals such as molybdenocene. Harding and co-workers reported the affinity or interaction of albumin with molybdenocene . [27] Similar studies have been carried out with other transition metals. Tinoco et al. reported the interaction

between Ti(IV) and HSA. This interaction was compared to that of Ti(IV) and transferrin where it was demonstrated that both routes of transport for Ti(IV) are feasible and that the most common binding of Ti(IV) is in the complex form and at different sites. The binding sites depended on the ligands coordinating Ti(IV). They concluded that titanocene dichloride binds HSA via hydrophobic sites. [28-29] This binding mechanism is through interaction of Cp rings or by direct coordination of the oxygen atoms in protein residues to the metal. Structure-activity studies, synthesis, studies and apotransferrin binding studies of Ti(IV) complexes have been carried out by Meléndez research group in the last 4 years. [30-31] They present that all the titanocene complexes synthesized have the ability to transfer Ti(IV) into the N- and C- lobes of transferrin . Regarding cytotoxicity, they found actives complexes where the IC_{50} for Cp_2TiCl_2, $[Ti_4(maltolato)_8(\mu\text{-}O)_4]$, $(Cp\text{-}COOEt)_2TiCl_2$ and $(Cp)(Cp\text{-}COOEt)TiCl_2$ were $4.5 * 10^{-4}$M, $2.8 * 10^{-4}$M, $5.8 * 10^{-4}$M and $6.3 * 10^{-4}$M respectively. On the other hand $(Cp\text{-}COOMe)_2TiCl_2$ and $(Cp)(Cp\text{-}COOMe)TiCl_2$ among others have shown to be not active. [31]

More recently, modified molybdenocenes with oxygen chelating ligands containing derivatives were synthesized. These modifications have the intention of exploring the role of the ancillary ligand and the cytotoxic properties of HT-29 and MCF-7 cancer cell line, and also the binding capabilities toward HSA. They found that maltolate and malonate ligands provide water-soluble molybdenocene complexes with higher stability than Cp_2MoCl_2 and that the improvement in their cytotoxic activities toward the HT-29 cell line was not very significant. However, it has been found that for MCF-7 cell line after 72 hours of drug exposure, they promote a proliferative behavior. [32]

Cyclic voltammetry (CV) studies on molydenocene complexes were conducted to measure the molybdenocene-DNA interaction [33]. The outcome of this study showed that molydenocene-DNA interaction is weak. Similar studies were pursued with HSA protein to determine the amount of binding interactions [32,34]. By conducting these studies it was found that there was a 15% of interaction between HSA and molybdenocene, suggesting that HSA is a powerful transporter for molybdenocene. Based on the above results, it was determined that the possible HSA-molybdenocene interaction was hydrophobic. Feliciano et. al. did not found a correlation between their ctotoxic activity and the binding affinity for HSA.

When comparing Cp_2MoCl_2 with other metallocene, molybdenocene has higher solubility in water and stability at physiological pH. Since molybdenum is present in significant amounts in the body having an important role in biochemistry, molydenocene dichloride and derivatives have great potential to become drugs. As a consequence, a great amount of molybdenum complexes have been prepared and used as model compounds to target specific biological activity and/or function. Considering the characteristics of molybdenum and taking them into account, we present a novel research that shows the development of a new synthetic methodology in aqueous solution of molybdenocene complexes containing thionucleobases/thionucleoside. The advantage of these complexes is that they are stable under physiological conditions and some of them present good anti-proliferative activity toward the HT-29 colon cancer cell and MCF-7 breast cancer cell lines. Also we report NMR and UV-VIS studies of the binding of molybdenocene to HSA.

1.1 Objectives

In order to reinforce our on-going efforts to determine the biological applications and anticancer properties of metallocenes complexes four new complexes will be synthesized and characterized with spectroscopic and spectrometric techniques. Their ability to interact with biological molecules and their *in vitro* activity in cancerous cells will also be studied.

The specific project aims can be summarized as follows:

1. To develop a novel procedure of preparing molybdenocene derivatives with different thionucleobase and thionucleoside ligands with the purpose of improving molybdenocene antitumor properties.
2. To characterize the prepared complexes with spectroscopic techniques such as NMR, UV and IR and spectrometric techniques such as MS and elemental analysis.
3. To study the novel molybdenocene interactions with Human Serum Albumin by ^{1}H NMR and UV spectroscopy.
4. To evaluate the cytotoxic activity of molybdenocene complexes in tumor cells such as HT-29 colon cancer cell line and MCF-7 human breast cancer cell line.

2. Experimental

2.1 Synthesis of [$Cp_2Mo(L)$]Cl (L = 6-Mercaptopurine, Mercaptopurine riboside, 2-amino-6-mercaptopurine, 2-amino-6-mercaptopurine riboside)

2.1.1 Materials

Molybdenum derivatives were synthesized with the starting material bis(cyclopentadienyl)molybdenum dichloride and the ligands, (-)-2-amino-6-mercaptopurine, 6-mercaptopurine, (-)-2-amino-6-mercaptopurine riboside and 6-mercaptopurine riboside, which were obtained from Aldrich. To be certain of the purity of the starting material and the ligands, ^1H NMR was used. Water was previously deionized, heated to eliminate carbonates and saturated with $N_{2(g)}$. Column chromatography was used to purify the molybdenocene-purine complexes. The stationary phase, Lipophilic Sephadex (20-100 μm), was purchased from Aldrich. Methanol, which assumed the mobile phase role, was purchased from Fisher.

2.1.2 Methods

A solution consisting of 0.050 g (0.17 mmol) of bis(cyclopentadienyl)-molybdenum dichloride and the equivalent mol amount of ligand was prepared in approximately 30 mL of previously heated and N_2 saturated distilled water, producing a brownish green solution. The solution pH was then adjusted to approximately 7.0 with 1.0 M NaOH and/or 1.0 M HCl. The reaction was carried out at room temperature in a three-neck round bottom flask equipped with a magnetic stirrer and under a nitrogen atmosphere (figure 5). Reaction time for [Cp_2Mo(6-mercaptopurine)]Cl and [Cp_2Mo(6-mercaptopurine ribose)]Cl were 18, 24 hours, respectively, and 48 hours for [Cp_2Mo((-)-2-amino-6-mercaptopurine)]Cl and [Cp_2Mo((-)-2-amino-6-mercaptopurine ribose)]Cl. The resulting orange solution was filtered through celite and the solvent removed under vacuum. Once dried, the solid was dissolved in methanol and filtered by

gravity. The filtrate was purified by column chromatography using lipophilic sephadex as stationary phase (figure 6) and methanol as mobile phase.

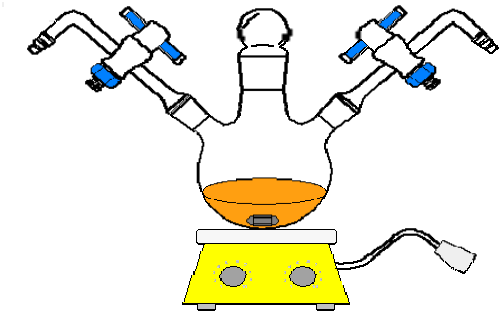

Figure 5 Schematic representation of the equipment used for the preparation of molybdenum derivatives

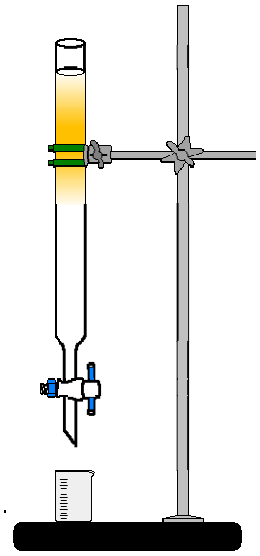

Figure 6 Schematic representation of the equipment used for the purification of molybdenum derivatives

2.2 Structure Characterization by Physical measurements

2.2.1 Materials and Methods

The chemical structures of the synthesized complexes were elucidated by the use of spectroscopic and spectrometric methods such as Nuclear Magnetic Resonance (NMR), Fourier Transform Infrared (FTIR), Mass Spectrometry (MS) and elemental analysis.

2.2.2 Nuclear Magnetic Resonance spectroscopy

NMR spectroscopy was used to determine the purity of the starting materials and ligands and the characterization of the isolated and purified complexes. For both purposes 90%H_2O:10%D_2O and DMSO were used as solvents. For characterization, solutions of 1.0×10^{-2}M were prepared for each of the complexes. For 1D experiment, the acquisition parameters were zgpr pulse program for water suppression. ^{1}H NMR spectra were recorded on a 500 MHz Bruker Advance NMR Spectrometer under controlled temperature at 25ºC and processed using a computer equipped with Linux software.

2.2.3 FTIR Spectroscopy

FTIR spectroscopy was used to identify the functional groups of the starting materials and the resulting complexes. All samples were recorded on a Bruker Vector-22 spectrophotometer as compressed KBr discs.

2.2.4 Mass Spectrometry

Approximately solutions of about 1 ppm were prepared using 0.2% v/v formic acid prior to mass spectral analysis. Electrospray positive ion was used as ionization mode. Mass spectrometry data were obtained on a Bruker Daltonics Esquire 6000 instrument. To determine the theoretical isotopic distribution pattern for the $[M - H]^+$ m/z peaks a Molecular Weight Calculator Program was used (available at http://jjorg.chem.unc.edu/personal/monroe).

2.2.5 Elemental Analysis

The elemental analyses were carried out by Atlantic Microlab, in Georgia.

2.3 Human Serum Albumin - Mo interactions

2.3.1 UV-VIS studies

2.3.1.1 Materials and Method

2.3.1.1.1 Buffer preparation

A physiological pH buffer (Tris buffer) was prepared for biological interaction studies. This buffer solution is used to prepare the protein solution as well as the solution for the complexes. Dionized water was heated and degasified before buffer preparation. Sodium chloride, sodium bicarbonate and tris(hydroxymethyl)aminomethane were dissolved in distilled/deionized water to produce concentrations of 100 mM, 10 mM and 10 mM, respectively. After dissolution the pH was adjusted to approximately 7.4 using 1.0 M NaOH and 1.0 M HCl, obtaining the Tris buffer solution.

2.3.1.1.2 HSA Solution

Human serum albumin (HAS) (99%) was obtained from Sigma-Aldrich (agarose gel electrophoresis, lyophilized powder) and used as purchased. A 1.0×10^{-5}M protein solution was prepared using Tris buffer solution at physiologic pH. The concentration of the protein solution was found by using the Beer-Lambert equation. For HSA the absorptivity coefficient at a wavelength of 280 nm is 35495 $M^{-1}cm^{-1}$.

2.3.1.1.3 Complex Solution

After the synthesis, characterization and purification process, a solution of 1.0×10^{-4} M of the complexes were prepared by dissolving the appropriate amount of the complex in the Tris buffer solution at physiologic pH.

2.3.1.1.4 Biological Interactions by UV/Vis Spectroscopy

UV/Vis spectroscopy measurements were obtained using a double beam Lambda BIO 20 Perkin–Elmer spectrophotometer thermostated at 25 ºC). The spectral data was recorded and analyzed using a 586 Nokia Computer System equipped with WinLab Software. For the human serum albumin - Mo interactions, approximately 2.0 mL 1.0×10^{-5} M of albumin solution was added to a UV/Vis quartz cell. An aliquot of the complex was added to the protein solution in the UV/Vis quartz cell and scanned in the wavelength region of 600 nm to 200 nm. This process was repeated 10 times in 45 minutes intervals. The pH in the UV/Vis quartz cell was monitored in every lecture to ensure that it was constant (7.4 ± 0.1).

2.3.2 NMR Studies

2.3.2.1 Materials and Methods

2.3.2.1.1 Buffer preparation

A physiological pH buffer was prepared for biological interaction studies. This buffer solution is used to prepare the protein solution as well as the solution for the complexes. A mixture of 90% H_2O:10%D_2O was used to prepare a solution of sodium chloride and Tris(hydroxymethyl-d_3)amino-d_2-methane (Tris-d_{11}) at concentrations of 100 mM and 10 mM, respectively. After dissolution the pH was adjusted to approximately 7.4 using 1.0 M NaOD and 1.0 M DCl, obtaining the Tris-d_{11} buffer solution.

2.3.2.1.2 HSA Solution

The human serum albumin (99%) was obtained from Sigma-Aldrich (agarose gel electrophoresis, lyophilized powder) and used as purchased. A 3.0 mM protein solution was prepared using Tris-d_{11} buffer solution at physiologic pH. As we mentioned the concentration of the protein solution was find out using the Beer-Lambert equation. For HSA the absorptivity coefficient at a wavelength of 280 nm is 35495 $M^{-1}cm^{-1}$.

2.3.2.1.3 Complex Solution

After the synthesis, purification and characterization process, a 1.0 mM complex solution was prepared by dissolving the appropriate molar amount of the complex in tris-d_{11} buffer solution at physiologic pH.

2.3.2.1.4 Biological Interactions

For the HSA-Mo interactions, 500 µL of 1.0×10^{-2} mM of albumin solution was added to the NMR tube. An aliquot of the complex was added to the protein solution. This process was repeated until a 1:2 ratio was obtained. The pH was monitored after and before the experiments to ensure that it was constant (7.4 ± 0.1). This experiment was done at 25ºC and 37ºC. For 1D experiments, the acquisition parameters were zgpr pulse program for water suppression. ^{1}H NMR spectra were recorded on a 500 MHz Bruker Advance NMR Spectrometer under controlled temperature and processed using a computer equipped with Linux software.

2.4 Cytotoxic Studies

2.4.1 Materials and Methods

All processes were done following aseptic techniques. This ensures that all cell culture procedures are performed to a standard that will prevent contamination from bacteria, fungi,

mycoplasma and cross contamination with other cell lines. All work was done under a tissue culture hood. The culture hood was sterilized using a UV light before any work was done in it. In the same manner, all equipment taken into the cabinet such as media bottles, pipette tip boxes and gloves were sprayed with 70% ethanol solution.

2.4.1.1 Medium Preparation

2.4.1.1.1 HT-29 Medium

McCoy's 5A Modified Media Formulation was purchased from American Type Culture Collection (ATCC). This medium was prepare by the supplier to contain 1.5 mM L-glutamine and 2.2g/L sodium bicarbonate. Fetal bovine serum (FBS) was purchased from ATCC. Antibiotic-antimyotic (AA) as well as Corning® bottle-top cellulose-acetate 0.2µm filters system were purchased from Sigma-Aldrich.

A volume of 50 mL of FBS and 5 mL of AA were added to the McCoy's 5A medium. The medium pH was adjusted to 7.4 using 1.0 M NaOH or 1.0 M HCl. This was followed by vacuum filtration using a bottle-top cellulose-acetate 0.2µm filter system in order to sterilize the medium.

2.4.1.1.2 MCF-7 Medium

Dubelcco's Modification of Eagle's Media (DMEM) was purchased from Cellgro. This medium is supplemented by supplier with L-glutamine, 4.5g/L glucose and sodium pyruvate. Fetal bovine serum (FBS) was purchased from ATCC. Antibiotic-antimyotic as well Corning® bottle-top cellulose-acetate 0.2µm filters system were purchased from Sigma-Aldrich.

In a bottle-top cellulose-acetate 0.2µm filter 450 mL of DMEM medium, 50 mL of 10% (v/v) fetal bovine serum and 5 mL of 1% (v/v) antibiotic-antimycotic were added and then filter in order to sterilize the medium.

2.4.1.2 Cells Line

3-(4,5-dimethylthiazol-2-yl)-2,5-diphenyltetrazolium bromide (MTT) viability assay where used to determine the cytotoxic activity of the molybdenocene complex. Two special cells lines where used to perform the viability assay, HT-29 colon cancer cells and MCF-7 breast cancer cells. HT-29 and MCF-7, both obtained from ATCC (ATCC HTB-38 and ATCC HTB-22). Both cell line were grown under 95% Air / 5% CO_2 (USP grade) atmosphere at 37 °C.

2.4.1.3 Complex Solution

A 10 mM complex's solution was prepared by dissolving the appropriate amount of the complex in DMEM medium and in McCOy's medium in order to dose MCF-7 and HT-29 cell line, respectively.

2.4.2 MTT Viability Assay

2.4.2.1 Materials

For the viability assay, MTT was purchased on Sigma-Aldrich, 96 well plates were purchased from VWR. Phosphate Buffer Solution (PBS) was prepared with sodium chloride, potassium chloride, sodium phosphate and potassium phosphate, all purchased from Sigma-Aldrich. Triton X-100 was obtained from Sigma and 2-propanol was purchased from Fisher.

2.4.2.2 Methods

MTT viability assay is a calorimetric assay for measuring the activity of enzymes that reduce MTT or MTS + PMS to formazan. MTT assays were performed into colon and breast cancer cell lines. A 100 µL suspension with an initial population of approximately 8,000 for HT-29 cells per well were seeded in a 96 well plate. For the MCF-7 cell line, an initial population of cells per well greater than that for the HT-29 was required because MCF-7 cells have a doubling time greater than HT-29. After 24 hours of incubation, a dose of the metal complex was added. Experiments were performed in quadruplicate plates. The plates were kept at 37°C in 95% air/5% CO_2 for 72 hours. Two hours before the completion of the 72 hours of incubation, a solution of MTT (1.0 mg/mL) was added and incubated. When time was completed and the purple formazan insoluble product was observed, the cell media was removed and plates were washed with cold PBS. The PBS was prepared with sodium chloride, potassium chloride, sodium phosphate and potassium phosphate dissolved in double distilled, deionized and autoclaved water. The PBS solution was autoclaved and filtered through cellulose-acetate 0.2µm filters. At this point 200 µL per well of a detergent solution, 10% (v/v) Triton X-100 in 2-propanol, was added and left at 37 °C in order to dissolve the formazan product. The absorbencies of the resulted colored solutions were measured at 570nm in the Micro Plate Reader with background subtraction at 630 nm. The instrument used was the 340 ATTC Microplate Reader from SLT Lab Instruments equipped with a temperature control unit and interfaced with a computer with WinSeLecT software. The IC_{50}, a metal complex concentration necessary to inhibit cell proliferation by 50%, was calculated by fitting the data to a four-parameter logistic plot using the Prism 3.0 software. All MTT protocol was performed in a dark room [40-41, 32]

3. Results and Discussion

3.1 Synthesis of Mo^{IV} Complexes

3.1.1 [Cp_2Mo(thionucleobases/thionucleoside)]Cl complexes

3.2 Structural characterization

3.2.1 FT-IR Analysis

3.2.1.1 [Cp_2Mo(6-mercaptopurine)]Cl

Infrared analysis was performed for [$Cp_2Mo(L)$]Cl complexes. Its spectrum was compared with Cp_2MoCl_2 and with the corresponding free ligand. This enabled us to make direct comparison of their functional groups and how they change upon coordination. Table 1 summarizes the IR data and Figures 1-3 present the IR spectra for comparison. The infrared spectrum of Cp_2MoCl_2 showed absorption bands at 3096 (s), 1426 (m), 830 (s) and 588 cm^{-1} (w) which corresponds to Cp ring C-H stretch, C=C stretch, C-H deformation and Mo-Cl stretch, respectively. The ligand 6-mercaptopurine has absorption bands at 3430 (s), 3099 (s), 1616 (s), 1580 (s), 1345(s) and 1224 cm^{-1} (s) which corresponds to N-H, C-H, C=N, C=C, C-N and S=C stretches, respectively. Once 6-mercaptopurine binds to Mo, the new complex exhibits absorption bands at 3315 cm^{-1} (N-H stretch), 3075 cm^{-1} (Cp ring C-H stretch), 1614 cm^{-1} (C=N stretch), 1421 cm^{-1} (Cp ringsC=C stretch), and 1330 cm^{-1} (C-N stretches), 522 cm^{-1} (Mo-N stretch) and 884 and 839 cm^{-1} for Cp C-H deformations.

The Cp C-H stretching absorption band in [Cp_2Mo(6-mercaptopurine)]Cl appears at lower energy compared to molybdenocene dichloride. Chloride ligands are σ and π donors, they donate electron density to the Mo through bonding and antibonding orbitals, respectively. On the other hand Cp rings donate σ to Mo and receive electron density from Mo through anti-

bonding orbitals. This means that the Cp rings in the molybdenocene dichloride are rich, or at least not deficient, in electron density due to the π-back donation from Mo. This effect makes the Cp C-H stretching frequency more energetic when is compared to the Cp C-H stretching of the product. The new chelate ring is able to make M-L π-back donation, thus decreasing the antibonding electron density from the Mo to the Cp rings. As a consequence the bond strength of the Mo-Cp increases due to the reduced Mo-Cp π-back donation. This means that the Cp C-H stretch becomes weaker as a consequence of poor electron density and decreases its wavenumber. There are also minor perturbations regarding C-S vibration. The band at 1224 cm^{-1}, attributed to C-S stretching decreases in intensity. This decrease in intensity of the C-S band has been accounted for as the substitution on sulfur by either a methyl group or metal coordination.[35,39]. In addition, around ca. 1600 cm^{-1}, the band corresponding to C=N decreases in intensity and while for C=C appears at lower wavenumber. These facts could indicate that the 6-mercaptopurine and its derivatives are likely to be engaged in a N(7) coordination to the Mo center, assisted by a S···Mo interaction[35-36]. To further establish this form of coordination through the sulfur of 6-thiopurine; the S-H bond is not observed in the infrared spectrum, suggesting that the ligand is in the thiolate form.

Table 1 FT-IR absorption frequencies for [Cp_2Mo(6-mercaptopurine)]Cl, 6-mercaptopurine and Cp_2MoCl_2

	Wavenumber (cm^{-1})		
Functional Group	[Cp2Mo(6-MP)]Cl	6-MP	Cp2MoCl2
ν(N-H)	3315	3430	-
ν(C-H), Cp	3075	-	3096
ν(C-H)	3083	3099	-
ν(C=N)	1614	1616 -	-
ν(C=C)	1570	1580	-
ν(C=C) , Cp	1421	-	1426
ν(C-N)	1330	1345	-
δ(C-H), Cp	884, 839	-	830
ν(S=C)	1224	1224	-
ν(Mo-N)	522	-	-
ν(Mo-Cl)	-	-	588

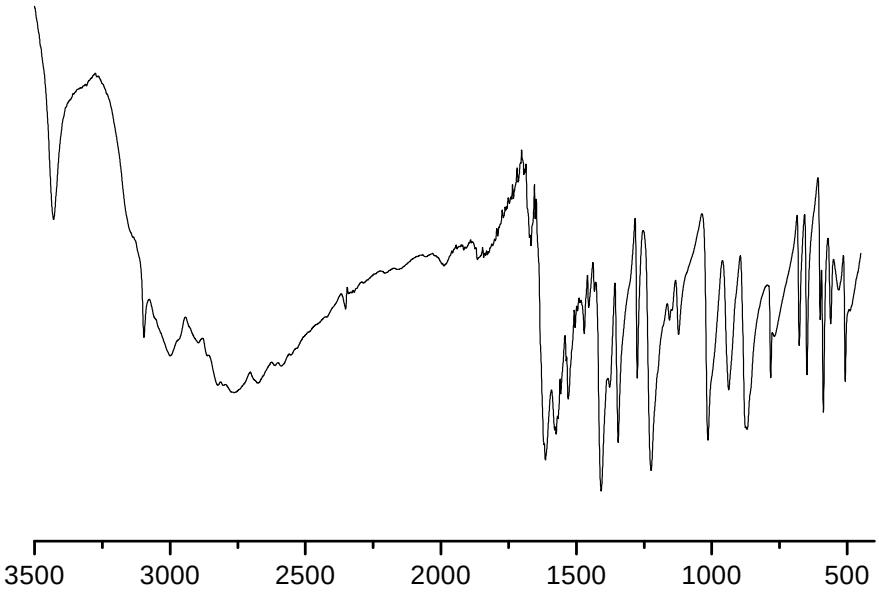

Figure 7 FT-IR spectra of 6-mercaptopurine in KBr pellet.

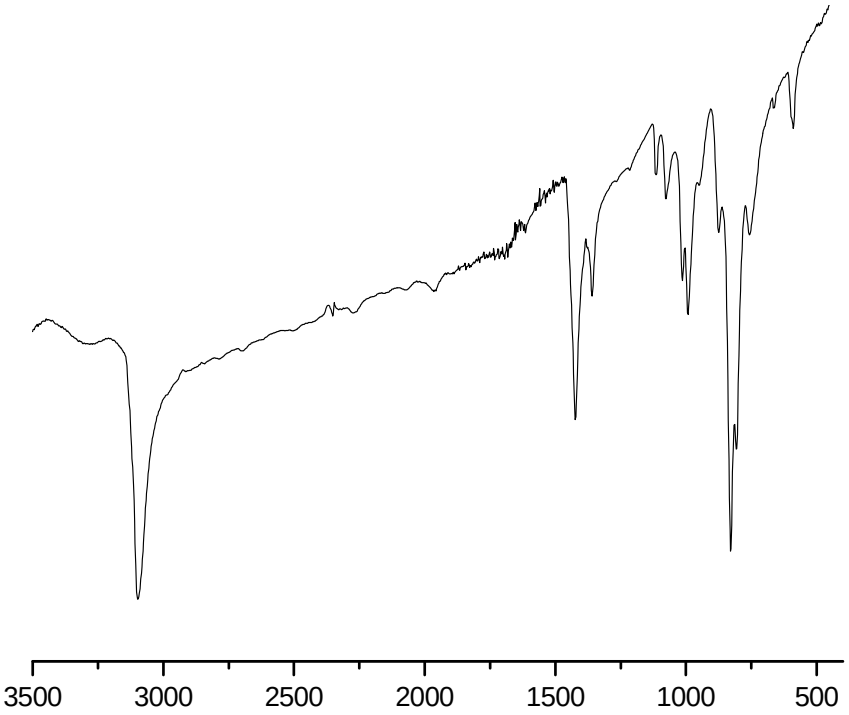

Figure 8 FT-IR spectra of Cp_2MoCl_2 in KBr pellet.

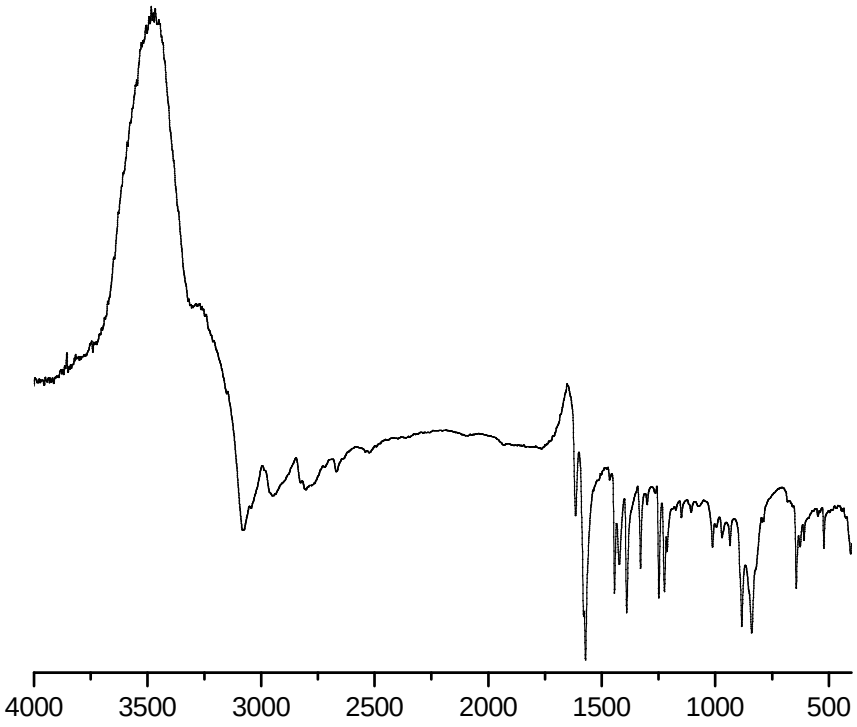

Figure 9 Infrared spectra of [CpMo[6-mercaptopurine]Cl in KBr pellet.

3.2.1.2 [Cp_2Mo(6-mercaptopurine ribose)]Cl

The IR spectral data for 6-mercaptopurine ribose, Cp_2MoCl_2 and the complex [Cp_2Mo(6-mercaptopurine ribose)]Cl have been analyzed and the corresponding bands to the new complex have been assigned, since they share almost the same functional groups as [Cp_2Mo(6-mercaptopurine)]Cl, see Table 2 . Thus it should exhibit similar spectral behavior. The 6-mercaptopurine ribose differs to 6-mercaptopurine on the presence of a ribose carbohydrate which has hydroxide, epoxide and alkyl groups which are not expected to have significant changes after ligand coordination to Mo(IV).

Table 2 FT-IR absorption frequencies for [Cp_2Mo(6-mercaptopurine ribose)]Cl, 6-mercaptopurine and Cp_2MoCl_2

	Wavenumber (cm^{-1})		
Functional Group	**[Cp2Mo(6-MPR)]Cl**	**6-MPR**	**Cp2MoCl2**
ν(N-H)	3386	3393	-
ν(C-H), Cp	3075	-	3096
ν(C-H)	2933	3122	-
ν(C=N)	1623	1602	-
ν(C=C)	1582	1547	-
ν(C=C) , Cp	1418	-	1426
ν(C-N)	1340	1336	-
δ(C-H), Cp	883, 840	-	830
ν(S=C)	1203	1211	-
ν(Mo-N)	490	-	-
ν(Mo-Cl)	-	-	588

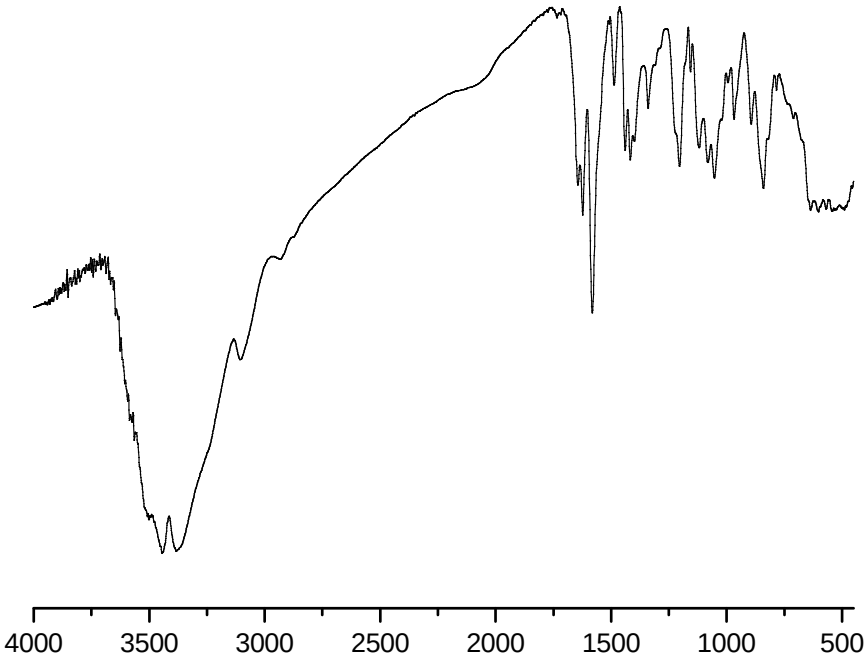

Figure 10 Infrared spectrum of [CpMo[6-mercaptopurineribose]Cl in KBr pellet.

3.2.1.3 [Cp_2Mo((-)-2-amino-6-mercaptopurine)]Cl

In analogous manner as the -6mercaptopurine complexes, IR spectral data for 2-amino-6-mercaptopurine, Cp_2MoCl_2 and [Cp_2Mo((-)-2-amino-6-mercaptopurine)]Cl have been analyzed allowing us to assign the band of the new species in the IR spectrum, see Figure 12 and Table 3. The (-)-2-amino-6-mercaptopurine differs to 6-mercaptopurine on the presence of an amine substituent at C(2), its absorption pattern is not expected to have a significant change after ligand coordination to Mo(IV). The rest of the thionucleobase contains the same functional groups as 6-mercaptopurine, thus the assignment has been straightforward. Since the spectral features of [Cp_2Mo(2-amino-6-mercaptopurine)]Cl over the 3000 cm^{-1} corresponding to NH_2 vibration is not well resolved, the exact band for this functional group versus the N(9)-H cannot be distinguished.

Table 3 FT-IR absorption frequencies for [Cp_2Mo((-)2-amino-6-mercaptopurine)]Cl, (-)-2-amino-6-mercaptopurine and Cp_2MoCl_2

	Wavenumber (cm^{-1})		
Functional Group	**[Cp_2Mo((-)2-A-6-MP)]Cl**	**(-)2-A-6-MP**	**Cp_2MoCl_2**
ν(N-H)	3289	3282	-
ν(C-H), Cp	3081	-	3096
ν(C-H)	2912	2945	-
ν(C=N)	1642	1666	-
ν(C=C)	1599	1634	-
ν(C=C) , Cp	1414	-	1426
ν(C-N)	1385	1374	-
δ(C-H), Cp	808	-	830
ν(S=C)	1257	1258	-
ν(Mo-N)	571	-	-
ν(Mo-Cl)	-	-	588

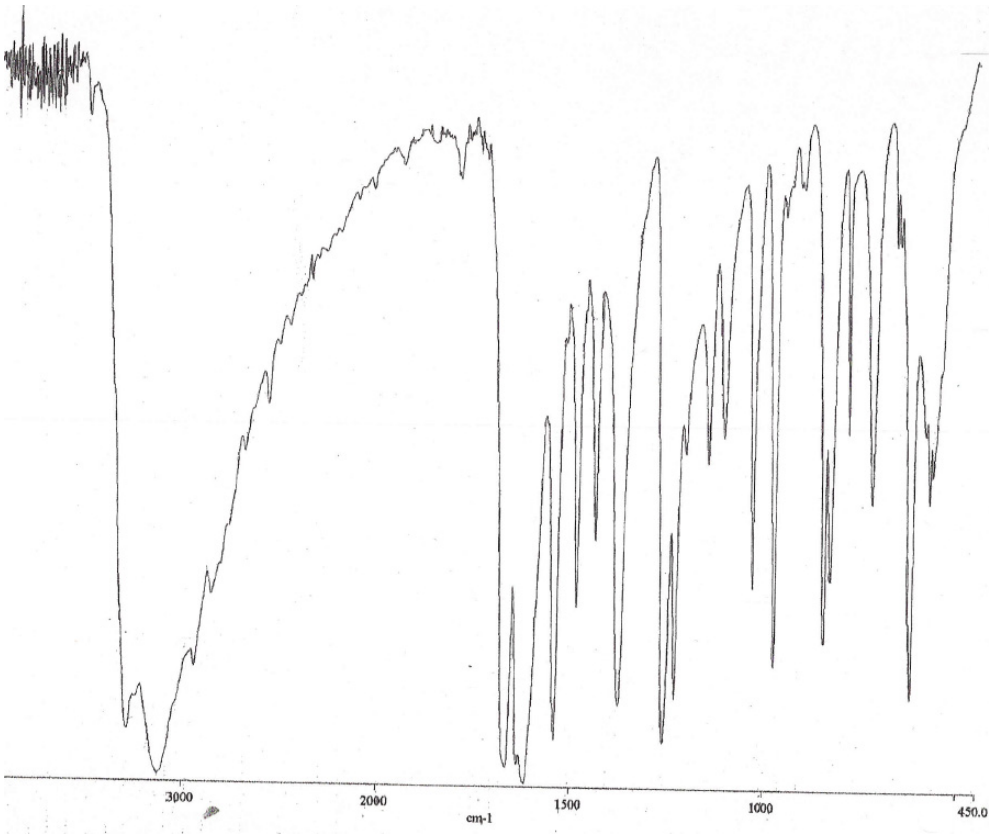

Figure 11 Infrared spectrum of (-)-2-amino-6-mercaptopurine in KBr pellet.

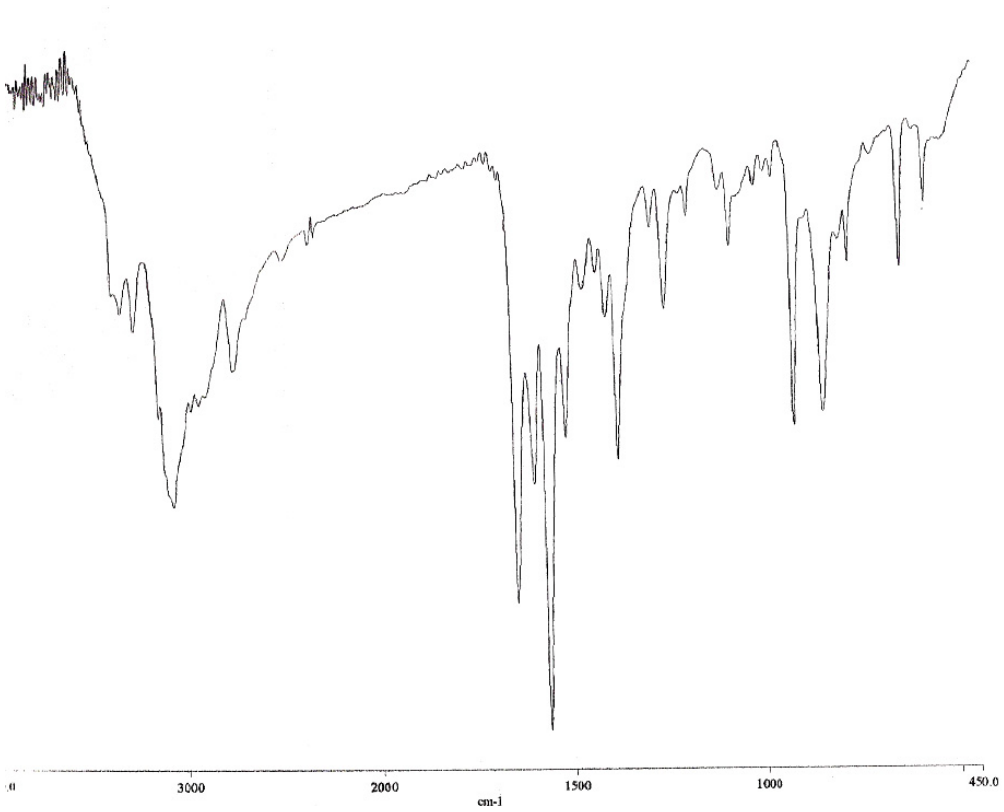

Figure 12 Infrared spectrum of [CpMo[(-)-2-amino-6-mercaptopurine]Cl in KBr pellet.

3.2.2 ^{1}H NMR Analysis

3.2.2.1 [Cp_2Mo(6-mercaptopurine)]Cl

3.2.2.1.1 [Cp_2Mo(6-mercaptopurine)]Cl in dimethyl sulfoxide-d_6

Spectral features of 6-mercaptopurine and its complex have been used to propose the structure of [Cp_2Mo(6-mercaptopurine)]Cl. The ^{1}H NMR spectrum in dimethyl sulfoxide-d_6 (DMSO-d_6) of 6-mercaptopurine shows one resonance singlet for the N-H(9) at 13.58 ppm and two singlet for H(2) and H(8) at 8.21 and 8.47 ppm, respectively. The ^{1}H NMR spectrum in dimethyl sulfoxide-d_6 (DMSO-d_6) of Cp_2MoCl_2 shows one resonance singlet for the C-H protons of the Cp ring at 5.53 ppm. It is known that 6-mercaptopurine can undergo tautomerism. Due to the reaction medium (pH = 7.4), during the reaction, the 6-mercaptopurine tautometers experience deprotonation at H(1), thus making reactive tautomeric resonance structures shown in Figure 13.

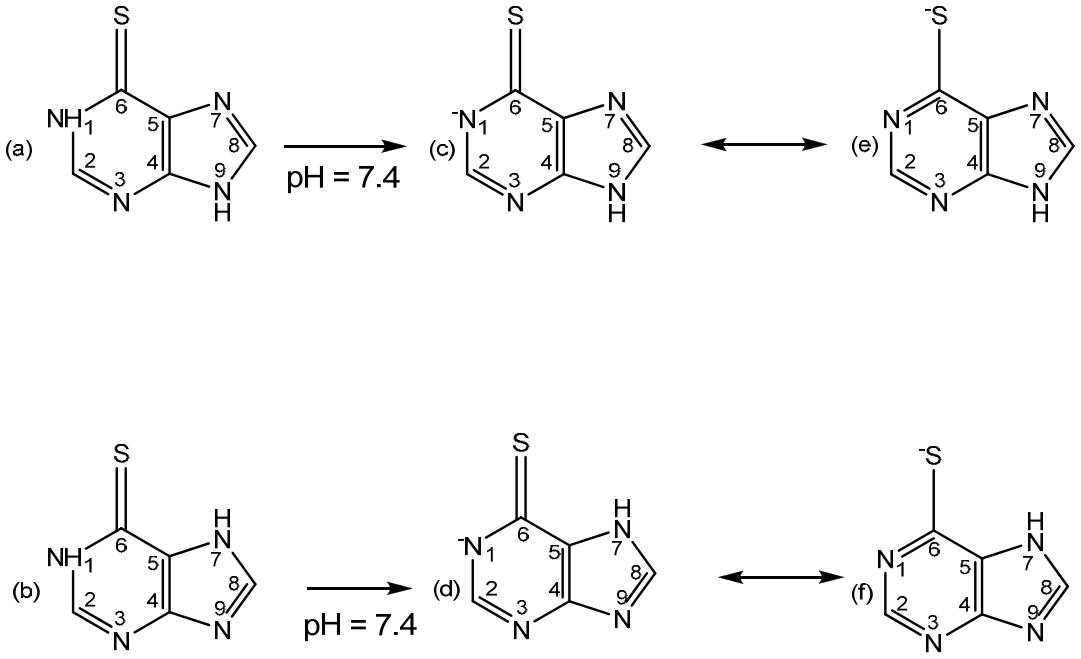

Figure 13 Tautomers (a) an (b) of 6-mercaptopurine and their deprotonated resonant structures (c), (d), (e) and (f) at pH values ≈ 7.4.

Of all the forms described in Figure 7, structure (e) is more likely to engage coordination to Mo (IV) forming two possible isomers. If Mo(IV) is coordinated by N(1) and S(6) it forms a 4-member chelate and if coordinated by N(7) and S(6) it forms a 5-member chelate, shown in Figure 15.

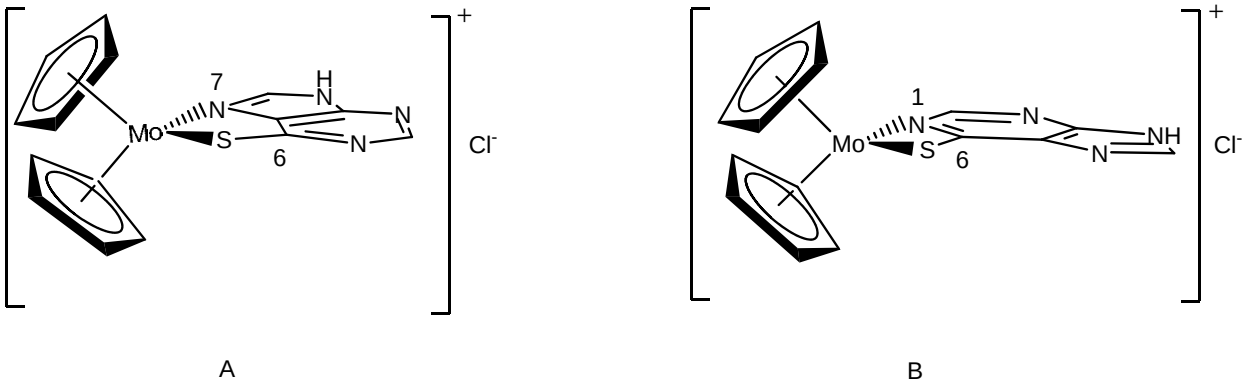

A B

Figure 14 Proposed 5-member chelate (a) and 4-member chelate isomer structures for $[Cp_2Mo(6\text{-mercaptopurine ribose})]^+$ in a pH = 7.4 aqueous medium.

Of these two possible isomers, we believe, based on thermodynamic consideration, that only the 5-member chelate is observed in the ^1H NMR spectrum in DMSO-d_6. The predominance of this structure might be explained by the stability of the 5-member chelate over the 4-member chelate. Five-member chelate species have been reported for Mo(IV) complexes with (-)-2-amino-6-mercaptopurine and 6-mercaptopurine ribose and for Ti(IV) complexes with (-)-2-amino-6-mercaptopurine and 6-mercaptopurine [35,37]. Since the reported complexes were prepared in methanol, deprotonation of H(1) was not observed and the complexes binding sites were attributed to be engaged through N(7) to the Ti center and an assisted weak interaction of S(6) and the Ti metal center.[35] The complex reported here undergoes deprotonation, most likely, of H(1), which then tautomerizes to the thiolate form (e) and lead to S(6), N(7) coordination. However, the S(6), N(1) coordination cannot be ruled out. When the reaction is

finished, the aqueous reaction medium is removed in order to obtain the solid product. The removal of the polar protic solvent medium apparently disfavors existence of the less stable 4-member chelate complex which is observed in very small quantity in the ^{1}H NMR spectrum in DMSO-d_6, since the solvent is aprotic. The polar protic medium enables the complex to bind to the Mo(IV) central metal through N(7) and S(6), and N(1) and S(6), the latter is less probable in an aprotic non-polar medium.

After coordination, the 6-mercaptopurine bound to Mo(IV) experiences a downfield shift for the N-H proton H(9) at 13.90 ppm and H(8) proton at 8.51 ppm and an upfield shift for H(2) at 8.01 ppm. The coordinated Cp also experiences a downfield shift at 5.70 ppm when compared to uncoordinated Cp. In [Cp_2Mo(6-mercaptopurine)]Cl protons H(9) and H(8) are deshielded since they fall under the Cp deshielding region. This deshielding region is due to the magnetic anisotropy induced to nearby protons by the Cp, produced by the circulating π electrons on the Cp ring. The second set of resonances, albeit in small quantities, should belong to the S(6), N(1) coordination.

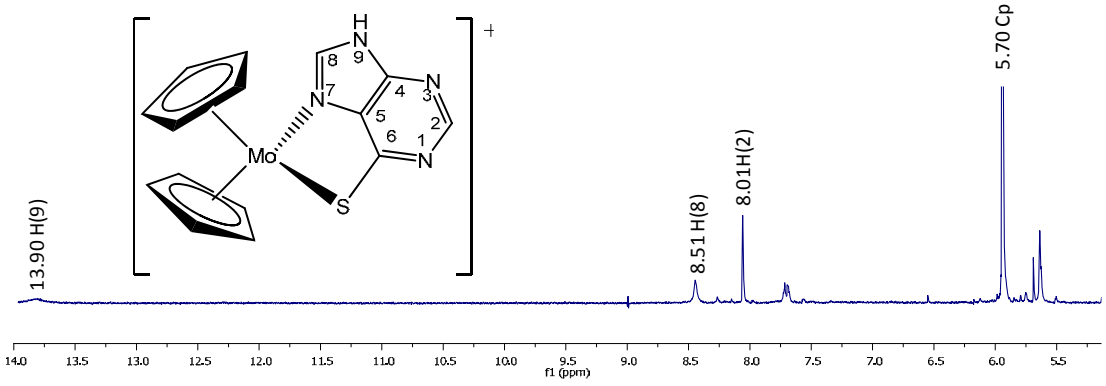

Figure 15 The 500MHz ^{1}H NMR spectra of [Cp_2Mo(6-mercaptopurine)]$^{+}$ in DMSO-d_6.

3.2.2.1.2 [Cp_2Mo(6-mercaptopurine)]Cl in 90%H_2O:10%D_2O

Spectral features of 6-mercaptopurine and its complex have been used to propose the structure of [Cp_2Mo(6-mercaptopurine)]Cl in aqueous environment. The ^1H NMR spectrum of Cp_2MoCl_2 in H_2O/D_2O shows two singlets for the C-H protons of the Cp ring at 5.79 and 5.97 ppm, shown in Figure 16. Two singlet signals of two different species are expected since it is well known that upon dissolution in aqueous medium, Cp_2MoCl_2 undergoes chloride hydrolysis. The two species formed are $Cp_2Mo(OD)(D_2O)^+$ and $Cp_2Mo(D_2O)_2^{2+}$ the latter been the most predominant at low pH. [37,45] This means that in the ^1H NMR spectrum of Cp_2MoCl_2 the)]Cl, shown in Figure 16, shows the presence of two isomers; where 6-mercaptopurine is coordinated to the Mo(IV) as a 4-member and 5-member chelate rings. The existence of these isomers was discussed in the previous section. Since the ^1H NMR spectrum was taken in an aqueous medium it resembles the reaction media where the two isomers coexisted. This means that three resonance singlet are expected for each isomer for a total six resonance peaks. The resonance singlet at 5.60, 7.83 and 8.30 ppm is attributed to the isomer bound to S(6) and to N(1) as a 4-member chelate ring. The singlets at 5.73, 7.78, and 8.21 ppm correspond to the isomer bound to S(6) and N(7) as a 5-member chelate ring. The attribution of H(2) resonance peak at 8.30 ppm (down shifted) in the 4-member chelate ring is due to the deshielding effect induced by the Cp magnetic anisotropy. This is compared to the more shielded resonance peak at 7.78 ppm for H(2) of the isomer with the 5-member chelate ring. In the same manner the resonance peak at 8.21 of H(8) is deshielded since it lies under the plane of the Cp magnetic anisotropy due to the 5-member chelate ring. This is compared to the more shielded resonance peak at 7.83 ppm of H(8) of the isomer with the 4-member chelate ring. The most intense resonance singlet peaks

were attributed to S(6), N(7) isomer since, the chelate is a 5-member ring and should be more thermodynamically stable, thus is more predominant.

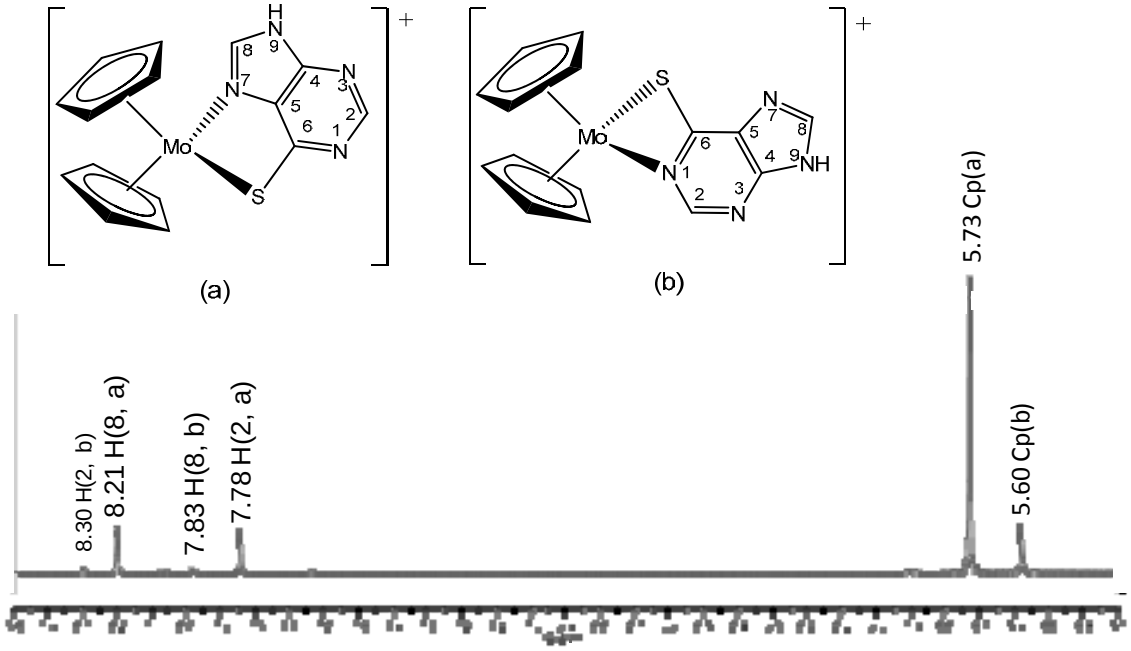

Figure 16 The 500MHz ^{1}H NMR spectra of [Cp_2Mo(6-mercaptopurine)]Cl isomers in 90%H_2O:10%D_2O.

3.2.2.2 [Cp_2Mo(6-mercaptopurine ribose)]Cl

3.2.2.2.1 [Cp_2Mo(6-mercaptopurine ribose)]Cl in dimethyl sulfoxide-d_6

Spectral features of 6-mercaptopurine, 6-mercaptopurine ribose and [Cp_2Mo(6-mercaptopurine)]Cl have been used to propose the structure of [Cp_2Mo(6-mercaptopurine ribose)]Cl. The ^{1}H NMR spectrum in dimethyl sulfoxide-d_6 (DMSO-d_6) of 6-mercaptopurine ribose (figure 18) shows one resonance singlet for the N-H proton H(9) at 13.82 ppm and two singlets for H(2) and H(8) at 8.22 and 8.54 ppm, respectively. The upfield proton signals from 6.5 – 4.5 ppm belong to the ribose. The ^{1}H NMR spectrum in dimethyl sulfoxide-d_6 (DMSO-d_6) of Cp_2MoCl_2 shows one resonance singlet for the C-H protons of the Cp ring at 5.53 ppm. During the reaction, 6-mercaptopurine ribose experiences deprotonation of H(1) due to the reaction medium (pH ≈ 7.4), thus making reactive resonance structures (figure 17). As described in the previous section, two types of isomers can form due to resonant (tautomeric) structures. This means that there are two types of bidentate ligand coordination of 6-mercaptopurine ribose Mo(IV) can be envisioned.

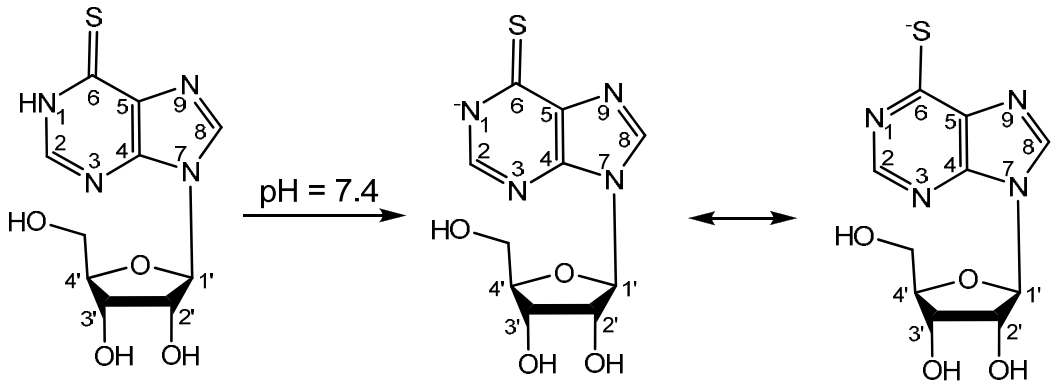

Figure 17 Deprotonation of 6-mercaptopurine ribose at pH ≈ 7.4 producing resonant structures.

After coordination, the Mo bound 6-mercaptopurine ribose shows similar spectral behavior to that of Mo bound to 6-mercaptopurine. The difference lies within H(9) which is not seen in this case. Thus the only protons observed other than those of the ribose are H(2) and H(8). Proton H(2) shifts upfield to 8.10 ppm and H(8) shifts downfield to 8.75 ppm compared to uncoordinated 6-mercaptopurine ribose. The coordinated Cp also experiences a downfield shift at 5.95 ppm when compared to uncoordinated Cp. Another species is evident in the ^{1}H NMR spectrum which is attributed to the S(6), N(1) coordination.

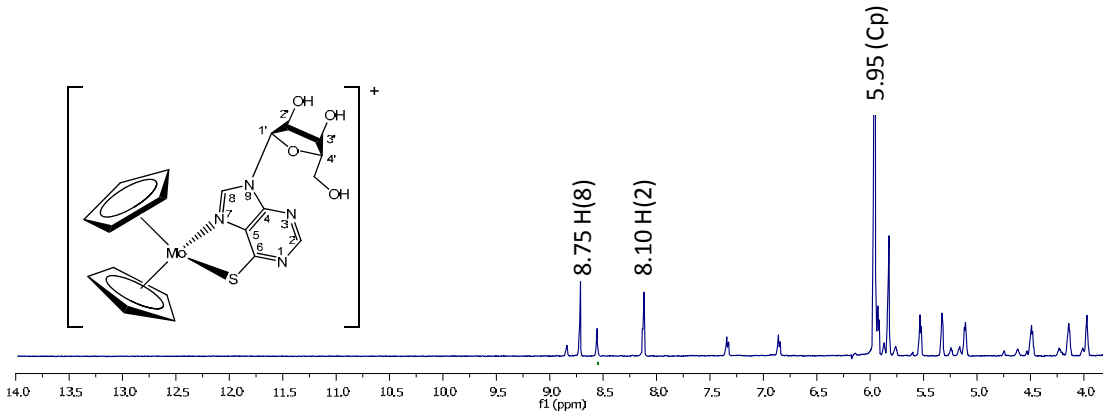

Figure 18 The 500MHz ^{1}H NMR spectra of $[Cp_2Mo(6\text{-mercaptopurine ribose})]^{+}$ in DMSO-d_6.

3.2.2.2.2 $[Cp_2Mo(6\text{-mercaptopurine ribose})]Cl$ in 90%H_2O:10%D_2O

Spectral features of 6-mercaptopurine, 6-mercaptopurine ribose and $[Cp_2Mo(6\text{-mercaptopurine})]Cl$ have been used to propose the structure of $[Cp_2Mo(6\text{-mercaptopurine ribose})]Cl$. As discussed in previous sections, two isomers are expected due to deprotonation of H(1) in aqueous media at pH ≈ 7.4, shown in Figure 19.

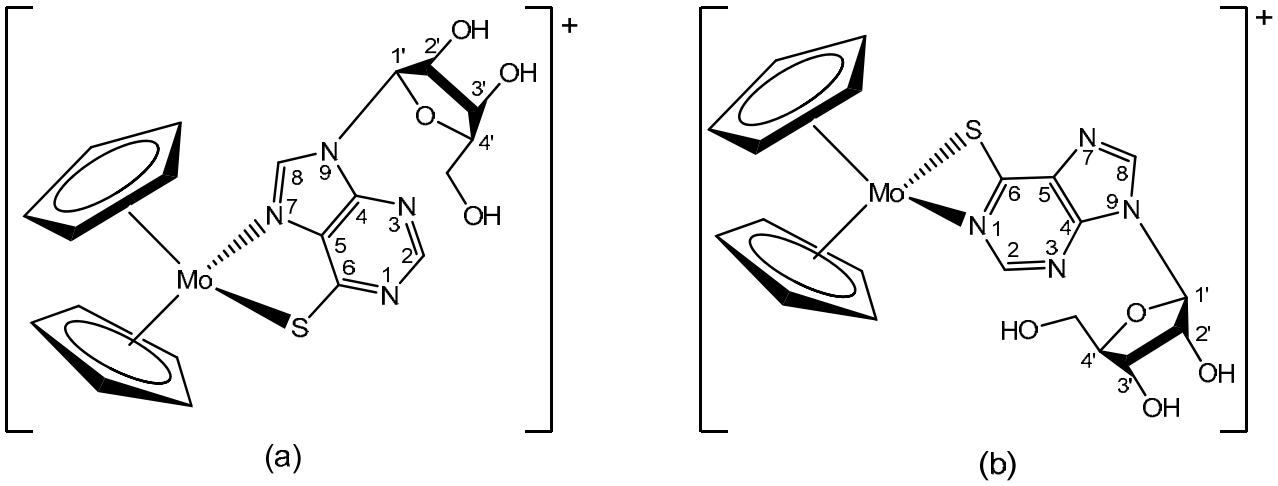

Figure 19 Proposed 5-member chelate (a) and 4-member chelate isomer structures for $[Cp_2Mo(6\text{-mercaptopurine ribose})]^+$ in a pH ≈ 7.4 aqueous medium.

The ^1H NMR spectrum in 90%H_2O:10%D_2O of 6-mercaptopurine ribose (figure 20) shows two singlets for H(2) and H(8) at 8.41 and 7.90 ppm, respectively for the predominant 5-member chelate. The classification of such signals is based on the fact that the most thermodynamically stable isomer should have the most intense signals. For the 4-member chelate singlets appear for H(2) and H(8) at 8.57 and 8.43 ppm, respectively. The coordinated Cp also experiences a downfield shift at 5.75 and 5.63 ppm for 5-member and 4-member chelates, respectively; when compared to uncoordinated Cp. The signals from 5.9 to 6.0 ppm are derived from the non-labile ribose protons. In $[Cp_2Mo(6\text{-mercaptopurine ribose})]Cl$ protons H(2) and H(8) are either shielded or deshielded due to the magnetic anisotropy induced to nearby protons by the Cp, produced by the circulating π electrons on the Cp ring.

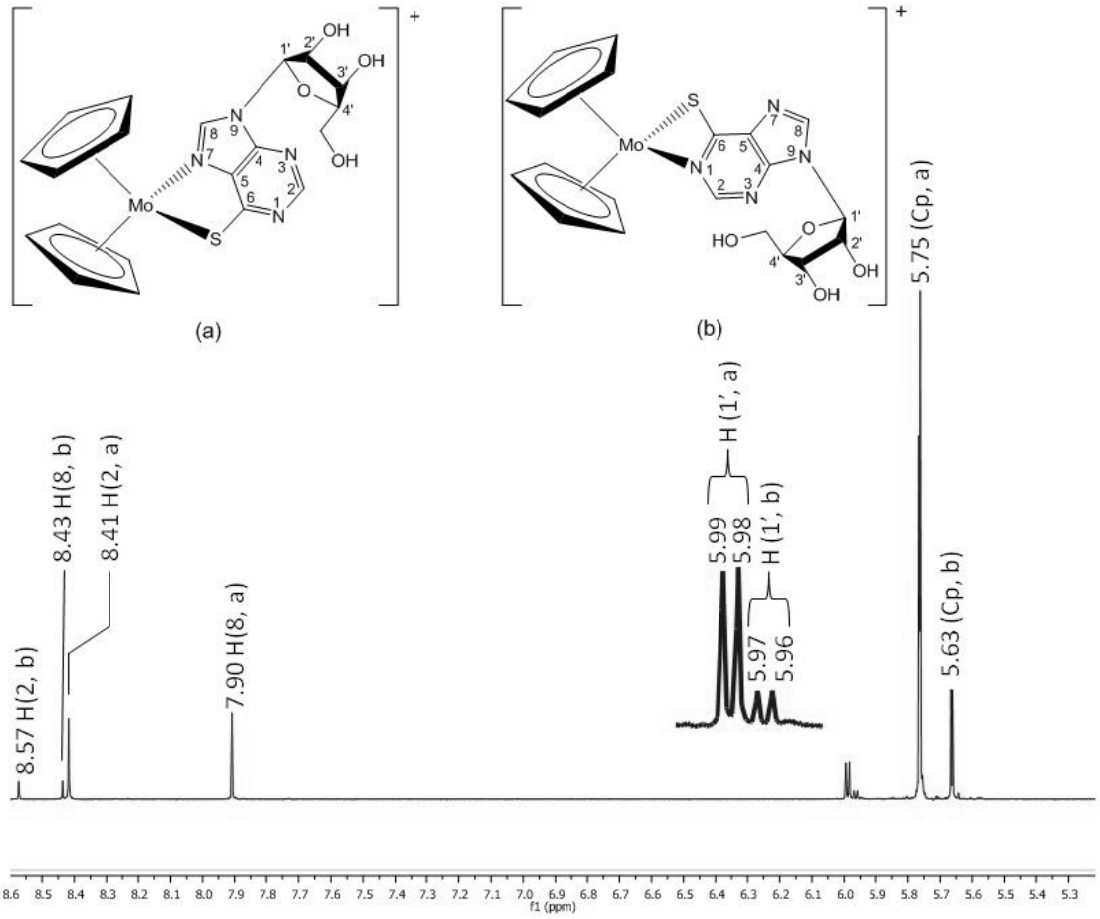

Figure 20 The 500MHz ^{1}H NMR spectrum of $[Cp_2Mo(6\text{-mercaptopurine ribose})]^{+}$ isomers in 90%H_2O:10%D_2O.

3.2.2.3 [Cp_2Mo((-)-2-amino-6-mercaptopurine)]Cl

3.2.2.3.1 [Cp_2Mo((-)-2-amino-6-mercaptopurine)]Cl in DMSO-d_6

Spectral features from 6-mercaptopurine, 2-amino-6-mercaptopurine and [Cp_2Mo(6-mercaptopurine)]Cl enabled the characterization of Cp_2Mo(2-amino-6-mercaptopurine)]Cl.

The ^1H NMR spectrum in DMSO-d_6 of (-)-2-amino-6-mercaptopurine in Figure 22 shows duplicate signal singlets due to the presence of two tautomers in a ratio of 1.2:0.8 that are not in thiol form as reported by Melendez et al. [35]

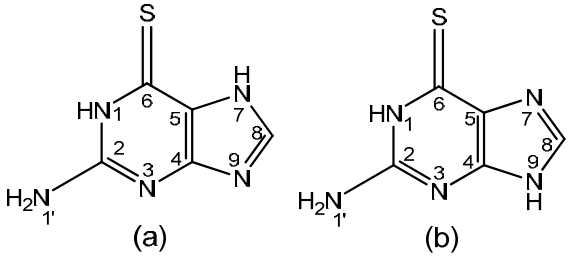

Figure 21 Tautomeric forms of 2-amino-6-mercaptopurine

Both tautomers show the N-H individual singlet resonances at 12.58 and 12.87 ppm assigned to the proton in N(1). The singlet signal at 12.01 and 11.83 ppm correspond to H(7) for tautomer (a) and H(9) for tautomer (b), respectively. The singlet signal at 8.10 and 7.82 ppm correspond to H(8) for tautomer (a) and H(8) for tautomer (b), respectively. The amino N-H_2(1') resonances appear at 6.62 ppm for tautomer (a) and 6.48 ppm for tautomer (b). The ^1H NMR spectrum in DMSO-d_6 of [Cp_2Mo((-)-2-amino-6-mercaptopurine)]Cl shows only one resonance singlet indicative of only one predominant isomer. The spectra in Figure 22 shows a singlet at 12.70 ppm assigned to H(9), a singlet at 7.97 ppm assigned to H(8), a broad singlet at 6.15 ppm assigned to N-H_2(1') and a singlet at 5.80 ppm assigned to the Cp protons. The coordinated Cp also experiences a downfield shift at 5.80 ppm when compared to 5.63ppm of the uncoordinated

Cp. This means that upon coordination, only one tautomer is recognized due to the singlet on N-H(9) resonance at 12.70 ppm, attributed to the thermodynamically stable 5-member chelate isomer.

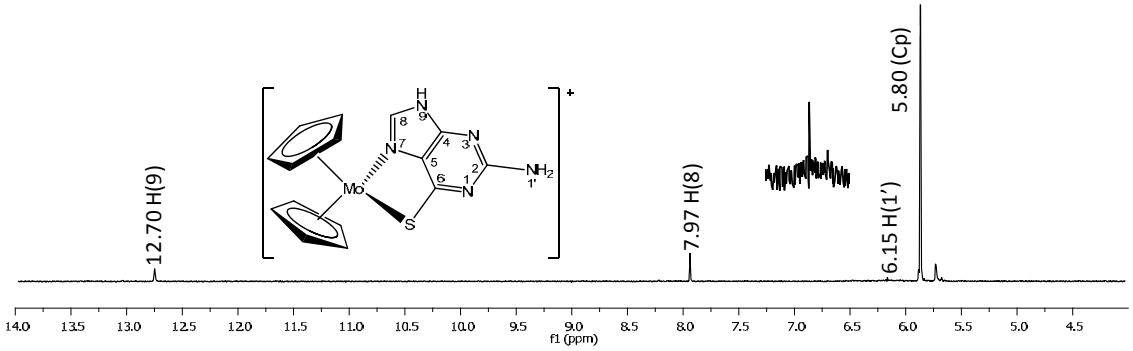

Figure 22 The 500 MHz ^{1}H NMR spectrum of $Cp_2Mo((-)$-2-amino-6-mercaptopurine)]Cl in dmso-d_6.

3.2.2.3.2 [Cp_2Mo((-)-2-amino-6-mercaptopurine)]Cl in 90%H_2O:10%D_2O

Spectral features of 6-mercaptopurine, 6-mercaptopurine ribose and [Cp_2Mo(6-mercaptopurine)]Cl have been used to propose the structure of [Cp_2Mo((-)-2-amino-6-mercaptopurine)]Cl. As discussed in previous sections, two isomers are expected due to deprotonation of H(1) in aqueous media at pH ≈ 7.4, shown in Figure 23.

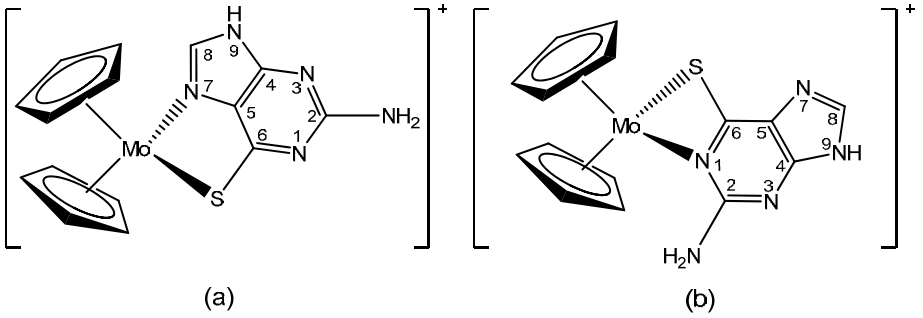

Figure 23 Proposed 5-member chelate (a) and 4-member chelate isomer structures for [Cp_2Mo((-)-2amino-6-mercaptopurine)]$^+$.

The ^{1}H NMR spectrum in 90%H_2O:10%D_2O of (-)-2-amino-6-mercaptopurine in Figure 24, shows a singlet for H(8) at 7.84 for the predominant 5-member chelate. The classification of such signals is based on the fact that the most thermodynamically stable isomer should have the most intense signals. For the 4-member chelate the singlet for H(8) appears at 7.65 ppm. The coordinated Cp also experiences a downfield shift at 5.75 and 5.55 ppm for 5-member and 4-member chelates, respectively; when compared to uncoordinated Cp. After purification the only the resonance peaks for the 4-member chelate complex diminish and those of the 5-member chelate complex are observed.

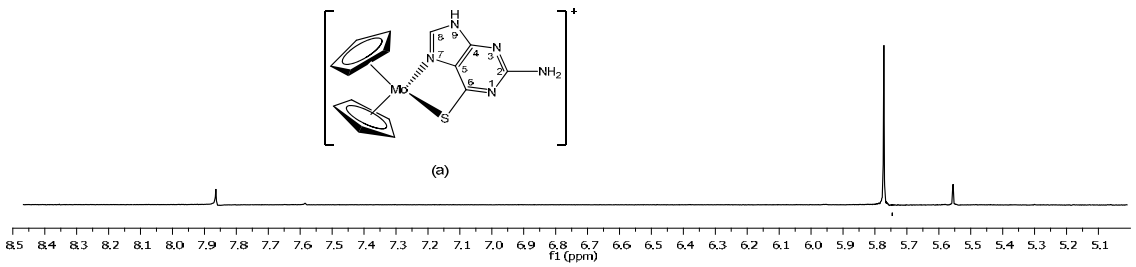

Figure 24 The 500 MHz ^{1}H NMR spectrum of 5-member ring chelate in 90%H_2O:10%D_2O.

3.2.2.4 [Cp_2Mo((-)-2-amino-6-mercaptopurine ribose)]Cl

3.2.2.4.1 [Cp_2Mo((-)-2-amino-6-mercaptopurine ribose)]Cl in dimethyl sulfoxide-d_6

Spectral features of 6-mercaptopurine ribose, (-)-2-amino-6-mercaptopurine and their respective complexes formed with the reaction with Cp_2MoCl_2 enabled the characterization of [Cp_2Mo((-)-2-amino-6-mercaptopurine ribose)]Cl.

The ^{1}H NMR spectrum in DMSO-d_6 of (-)-2-amino-6-mercaptopurine ribose, in Figure 25, shows a broad singlet at 6.80 ppm of the amino protons in N-H_2(1"), a singlet at 8.14 ppm of H(8) and a broad singlet at 11.95 ppm of H(1). The signals upfield from 6.0 ppm are derived from the ribose. The ^{1}H NMR spectrum in dmso-d_6 of [Cp_2Mo((-)-2-amino-6-mercaptopurine ribose)]Cl in Figure 25, shows two new singlet peaks at 6.57 and 6.64 ppm corresponding to the amino protons of the 4-member and 5-member chelate, respectively. These signals have shifted upfield when compared to the free ligand. It also shows two singlet peaks at 8.25 and 8.44 ppm corresponding to H(8) of the 5-member and 4-member chelate, respectively. These signals have shift downfield when compared to the free ligand. The Cp protons have shifted downfield from 5.53 ppm to 5.78 and 5.90 ppm for 4-member and 5-member chelate, respectively.

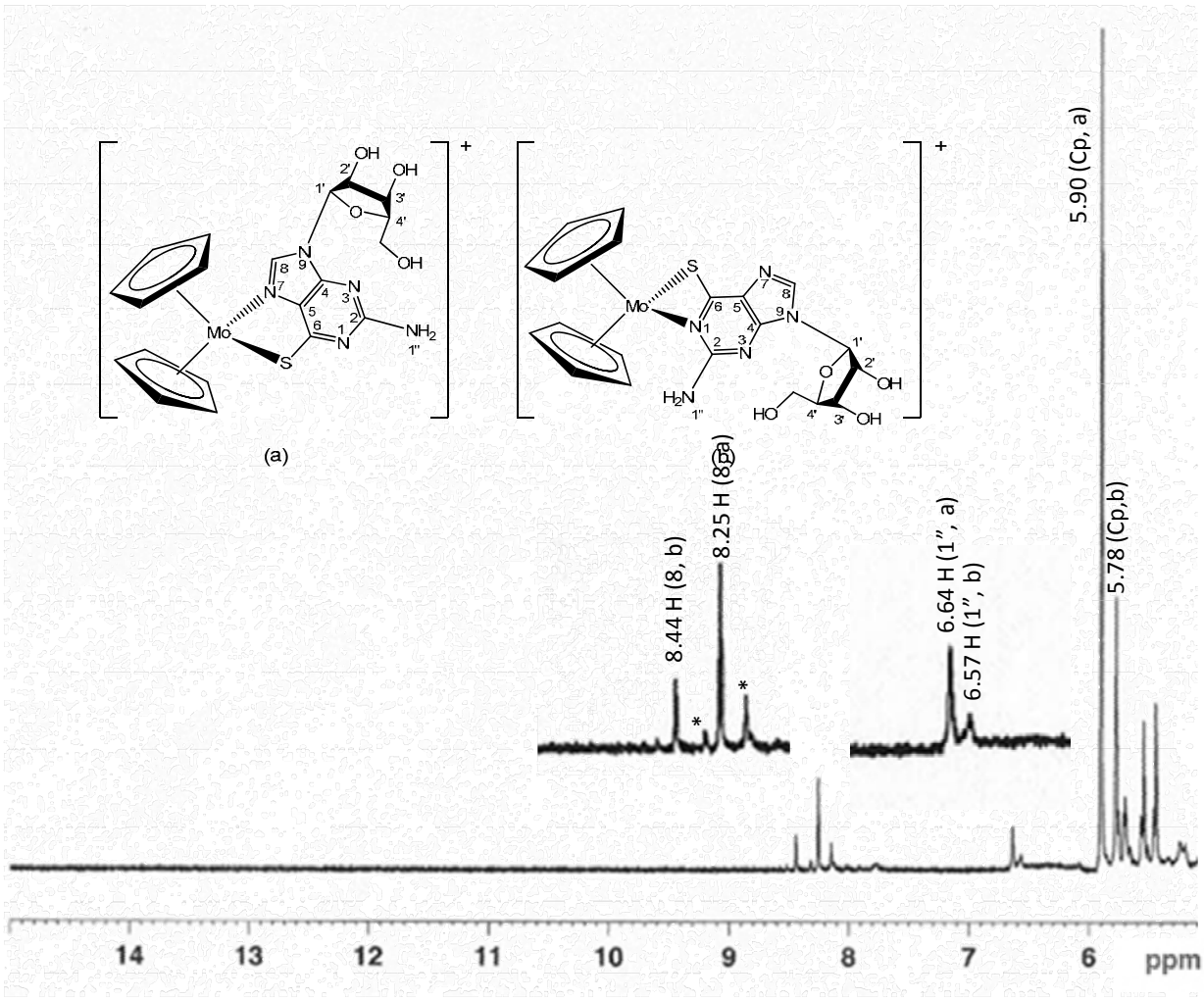

Figure 25 The 500MHz ^{1}H NMR spectrum of [Cp_2Mo((-)-2-amino-6-mercaptopurine ribose)]Cl isomers in dmso-d_6.

3.2.2.4.2 [Cp_2Mo((-)-2-amino-6-mercaptopurine)]Cl in 90%H_2O:10%D_2O

Spectral features of 6-mercaptopurine ribose, (-)-2-amino-6-mercaptopurine and their respective complexes formed with the reaction with Cp_2MoCl_2 enabled the characterization of [Cp_2Mo((-)-2-amino-6-mercaptopurine ribose)]Cl.

The ^{1}H NMR spectrum in 90%H_2O:10%D_2O of (-)-2-amino-6-mercaptopurine ribose, in Figure 26, shows a broad singlet at 6.80 ppm of the amino protons in N-H_2(1"), a singlet at 8.14 ppm of H(8) and a broad singlet at 11.95 ppm of H(1). The ^{1}H NMR spectrum in 90%H_2O:10%D_2O of [Cp_2Mo((-)-2-amino-6-mercaptopurine ribose)]Cl in Figure 26, shows a broad peak at 5.95 ppm which is attributed to the solvent-interchangeable amino protons of the two product isomers. It also shows two singlet peaks at 8.02 and 8.14 ppm corresponding to H(8) of the 5-member and 4-member chelate, respectively. The Cp protons have shifted upfield 5.97 ppm to 5.63 and 5.77 ppm for 4-member and 5-member chelate, respectively. The signals upfield from 5.5 ppm are derived from the ribose and are not shown in the spectrum.

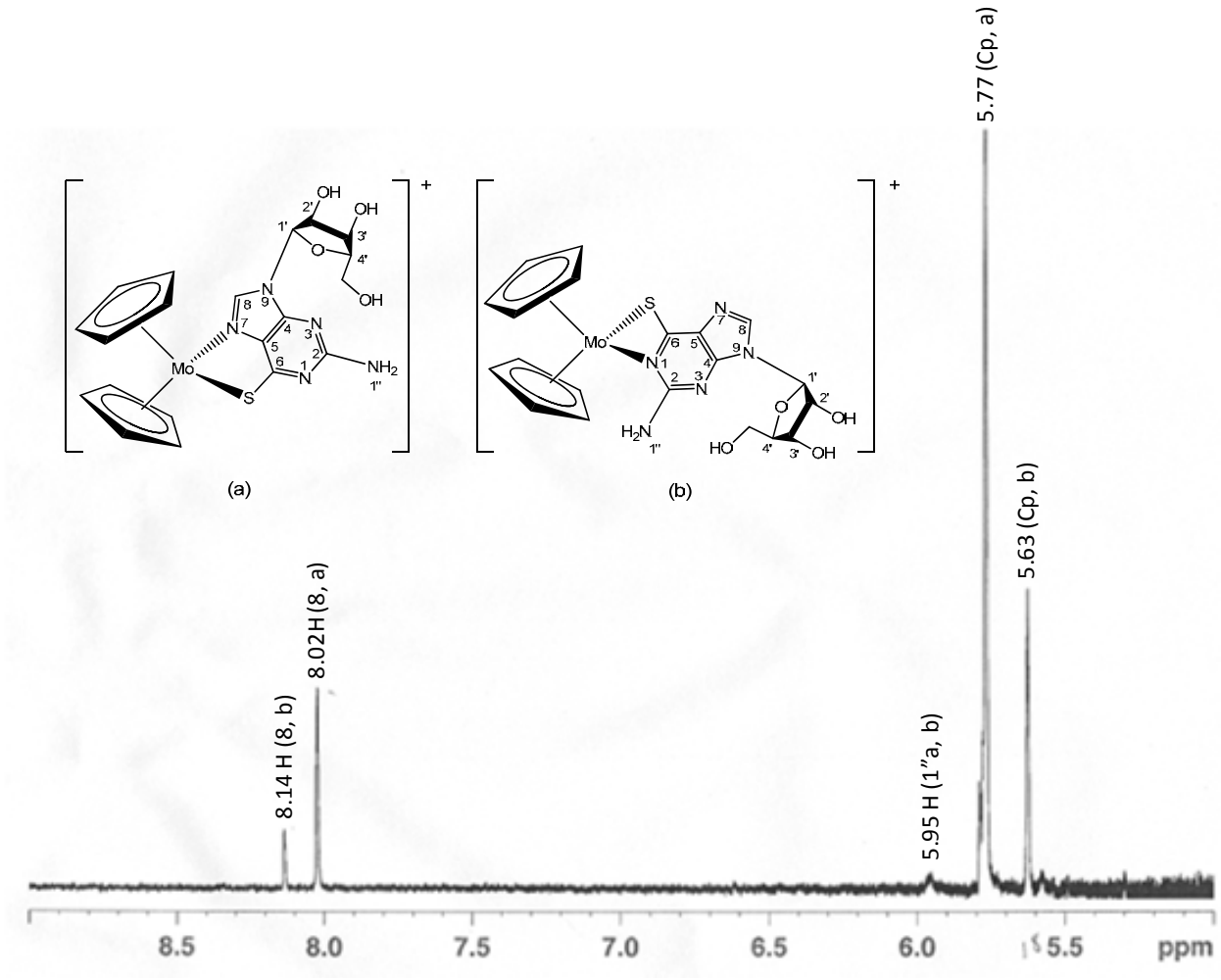

Figure 26 The 500MHz ^{1}H NMR spectrum of [Cp_2Mo((-)-2-amino-6-mercaptopurine ribose)]Cl isomers in 90%H_2O:10%D_2O

3.2.3 Mass Spectrometric Analysis

3.2.3.1 [Cp_2Mo(6-mercaptopurine)]Cl

Mass spectrometric analysis was perform to the new complex in order to determine the isotopic distribution pattern for the $[M\ ]^+$ m/z peaks using electrospray positive ion mode in presence of formic acid. The theoretical m/z peaks corresponding to $[Cp_2Mo$(6-mercaptopurine)$]^+$ is 379.0 which is in accordance with the experimental findings of m/z = 379. These results suggest that a +1 charged species $[Cp_2Mo$(6-mercaptopurine)$]^{+1}$ is formed for $[Cp_2Mo$(6-mercaptopurine)]Cl complex. The theoretical mass spectrometric isotopic distribution for $[Cp_2Mo$(6-mercaptopurine)$]^+$ was calculated using Molecular Weight Calculator Program available on http://jjorg.chem.unc.edu/personal/monroe and compared with the experimental one. The predicted molecular ion peak distributions are in fact observed experimentally in the recorded mass spectra. Accordingly, the mass spectrometric experimental data support the chemical composition projected for $[Cp_2Mo$(6-mercaptopurine)$]^+Cl^-$. The MS of $[Cp_2Mo$(6-mercaptopurine ribose)]Cl also corroborates and support the proposed formula for this new species. Results are shown in Table 4. Similar analysis was performed to $[Cp_2Mo$(6-mercaptopurine ribose)]Cl corroborating the proposed formula. Results are shown in Table 6.

Table 4 Isotopic abundance of $[Cp_2Mo(6\text{-mercaptopurine})]^+$

m/z	Experimental I (%)	Theoretical I (%)
373.1	49.03	54.76
374.1	8.57	10.25
375.1	33.81	37.52
376.0	59.38	65.63
377.0	71.26	74.7
378.0	51.55	50.7
379.0	100.00	100
380.0	18.14	19.45
381.0	41.71	41.41
382.0	6.94	7.49

Table 5 Isotopic abundance of $[Cp_2Mo(6\text{-mercaptopurine ribose})]^+$

m/z	Experimental I (%)	Theoretical I (%)
514	11	9.71
513	40	41.98
512	24	24.73
511	100	100
510	55	53.63
509	78	76.03
508	68	65.51
507	39	37.27
506	12	12.88
505	50	52.85

3.2.3.2 $[Cp_2Mo((-)\text{-2-amino-6-mercaptopurine})]Cl$

Mass spectrometric analysis was perform to the new complex in order to determine the isotopic distribution pattern for the $[M]^+$ m/z peaks using electrospray positive ion mode in presence of formic acid. The theoretical m/z peaks corresponding to $[Cp_2Mo(2\text{-amino-6-}$

mercaptopurine)]$^{+}$ is 394 which is with accordance with the experimental findings of m/z = 394. According to the elemental analysis and the mass spectrometric analysis these results suggest that a +1 charged species [Cp_2Mo(2-amino-6-mercaptopurine]$^{+1}$ is formed for [Cp_2Mo((-)-2-amino-6-mercaptopurine)]Cl complex. The theoretical mass spectrometric isotopic distribution for [Cp_2Mo((-)-2-amino-6-mercaptopurine)]$^{+}$ was calculated using Molecular Weight Calculator Program available on http://jjorg.chem.unc.edu/personal/monroe and compared with the experimental one. The predicted molecular ion peak distributions are in fact observed experimentally in the recorded mass spectra. Accordingly, the mass spectrometric experimental data support the chemical composition projected for [Cp_2Mo((-)-2-amino-6-mercaptopurine)]Cl. Similar analysis was performed to [Cp_2Mo((-)-2-amino-6-mercaptopurine ribose)]Cl corroborating the proposed formula. Results are shown in Table 5.

Table 6 Isotopic abundance of [Cp_2Mo((-)-2-amino-6-mercaptopurine)]$^{+}$

m/z	Experimental I (%)	Theoretical I (%)
388.1	55.71	54.66
389.1	10.42	10.43
390.1	36.82	37.48
391.1	67.95	65.64
392.1	81.29	74.81
393.1	53.75	50.88
394	100.00	100.00
395	18.66	19.78
396	40.09	41.41
397	7.34	7.63

Table 7 Isotopic abundance of $[Cp_2Mo((-)\text{-}2\text{-amino-}6\text{-mercaptopurine ribose})]^+$

m/z	Experimental I (%)	Theoretical I (%)
520.1	48.86	53.70
521.1	11.66	13.00
522.1	40.61	36.20
523.1	69.42	66.40
524.1	79.22	76.50
525.1	55.21	53.10
526.1	100.00	100.00
527	23.25	24.20
528	40.05	40.50
529	9.67	8.00

3.2.4 Elemental Analysis

3.2.4.1 $[Cp_2Mo(6\text{-mercaptopurine})]Cl$

After the synthesis and purification approximately 0.005g of the new molybdenocene complex was sent to Atlantic Microlab to corroborate the composition of the $[Cp_2Mo(6\text{-mercaptopurine})]Cl$. The elemental analysis suggests that the complex keep the two cyclopentadienyl groups and has only one chloride. The theoretical composition was obtained taking into account the possibility of the presence of a water molecule. This results support the molecular formula for this new complex. Results are shown in Table 6.

Table 8 Percent of composition of $[Cp_2Mo(6\text{-mercaptopurine})]Cl\bullet H_2O$

$[Cp_2Mo(6\text{-mercaptopurine})]Cl\cdot H_2O$		
Atom	**Theoretical (%)**	**Experimental (%)**
C	41.82	41.82
H	3.51	3.62

3.2.4.2 [Cp_2Mo(6-mercaptopurine ribose)]Cl

After the synthesis and purification approximately 0.005g of the new molybdenocene complex was sent to Atlantic Microlab to corroborate the composition of the [Cp_2Mo(6-mercaptopurine)]Cl. The elemental analysis suggests that the complex keep the two cyclopentadienyl groups and has only one chloride. The theoretical composition was obtained taking into account the possibility of the presence of a water molecule. This results support the molecular formula for this new complex. Results are shown in Table 6.

Table 9 Percent of composition of [Cp_2Mo(6-mercaptopurine)]Cl•H_2O

[Cp_2Mo(6-mercaptopurine ribose)]Cl·3 H_2O		
Atom	**Theoretical (%)**	**Experimental (%)**
C	40.11	40.43
H	4.54	4.18

3.2.4.3 [Cp_2Mo((-)-2-amino-6-mercaptopurine)]Cl

After the synthesis and purification approximately 0.005g of the new molybdenocene complex was sent to Atlantic Microlab to corroborate the composition of the [Cp_2Mo((-)-2-amino-6-mercaptopurine)]Cl. The elemental analysis suggests that the complex keep the two cyclopentadienyl groups and has only one chloride. The theoretical composition was obtained taking into account the possibility of the presence of a water molecule. This results support the molecular formula for this complex. Results are shown in Table 7.

Table 10 Percent of composition of [Cp_2Mo((-)-2-amino-6-mercaptopurine)]Cl•H_2O

[Cp_2Mo((-)-2-amino-6-mercaptopurine)]Cl·$2H_2O$		
Atom	**Theoretical (%)**	**Experimental (%)**
C	3.83	38.89
H	3.91	3.67

3.2.4.4 [Cp_2Mo((-)-2-amino-6-mercaptopurine ribose)]Cl

After the synthesis and purification approximately 0.005g of the new molybdenocene complex was sent to Atlantic Microlab to corroborate the composition of the [Cp_2Mo((-)-2-amino-6-mercaptopurine ribose)]Cl. The elemental analysis suggests that the complex keep the two cyclopentadienyl groups and has only one chloride. The theoretical composition was obtained taking into account the possibility of the e presence of a water molecule. This results support the molecular formula for this complex. Results are shown in Table 8.

Table 11 Percent of composition of [Cp_2Mo((-)-2-amino-6-mercaptopurine ribose)]Cl•H_2O

[Cp_2Mo((-)-2-amino-6-mercaptopurine Ribose)]Cl·$2H_2O$		
Atom	**Theoretical (%)**	**Experimental (%)**
C	40.3	40.2
H	4.3	4.1

3.3 Studies of the interactions of HSA with molybdenum dihalides complexes

3.3.1 U V-Vis Studies

Interaction studies between HSA and molybdenum dihalide were carried out with UV-Vis spectroscopy. This technique serves as a good tool since aromatic amino acid such as tryptophan and tyrosine absorb ultraviolet light. These amino acids have a strong characteristic maximum absorbance wavelength around 280 nm. Thus making UV-Vis spectroscopy an effective tool for determining protein concentrations with their Mo(IV) interactions.

The interaction study was carried out motoring the absorbance from 600 to 200 nm while performing a titrimetric analysis of HSA and molybdenocene dichloride, both in Tris buffer solution. Aliquots of the metal solution were added to the protein solution placed on a UV-Vis quartz cell until a ratio of 1: 10 (Human serum albumin: molybdenocene) was obtained. It was observed that the only absorption band present was at 280 nm which corresponds to the protein. This band did not diminish or increased from its baseline throughout the titration process. In addition, no new absorption bands or isosbestic points were present in the spectra.

Based on this information, no interaction is observed between the free species HSA and molybdenocene dichloride, or at least it cannot be detected by UV-Vis spectroscopy.

3.3.2 NMR Studies

The coordination of Cp_2MoCl_2 and their derivative complexes to the Human Serum Albumin were investigated by 1H NMR. In a NMR tube equivalents amount of molybdenum complexes in $tris_d$ buffer solution and HSA in $tris_d$ buffer solution were reacted at physiological pH. The conditions of this experiment where similar to those done in UV-Vis. A singlet was observed at 5.65 ppm, which is a different behavior when compared to the 1H NMR spectrum of molybdenocene dichloride in 90%H_2O:10%D_2O. This signal has been attributed to $Cp_2Mo(OD)(D_2O)+$ [37], since the complex is not in a H_2O:D_2O solution only. The buffer can have some degree of interaction with the complex, this apparent interaction might be so insignificant that no signal for this type of complex is not observed.

One equivalent of the protein was added to the NMR tube, it was left to react for 15 minutes at 25°C and no chemical shift was observed, see Figure 27. After 24 hours still no chemical shift was observed. This experiment was further done at a temperature of 37°C and no change in chemical shift was observed as well, Figure 28. The chemical shift was affected by a shift of $\Delta\delta = 0.19$ ppm between the two temperatures. This shift goes downfield for a temperature of 37°C and is attributed to the temperature change.

Molybdenocene complexes showed the same behavior tan those of molybdenocene dichloride. These experiments suggest that no interaction is observed between HSA and molybdenocene dichloride and molybdenocene complexes, or at least this interaction cannot be detected by NMR spectroscopy.

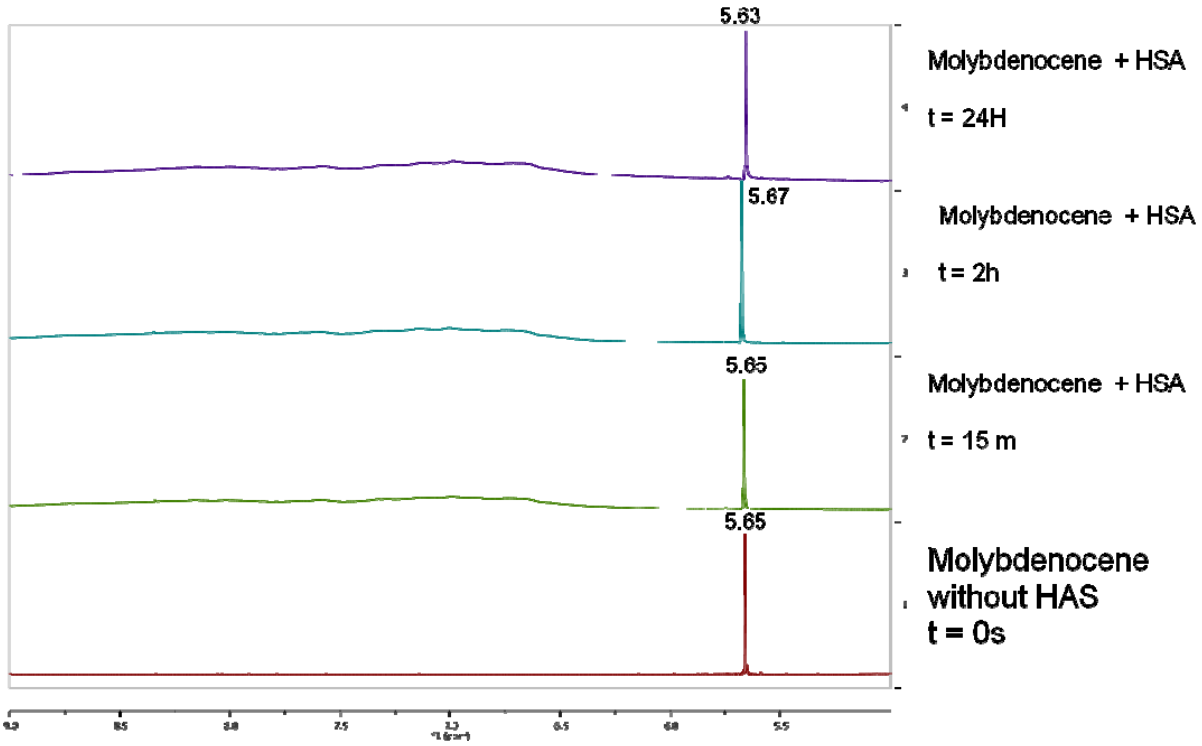

Figure 27 The 500MHz ^{1}H NMR spectra at different time intervals of the interaction of Cp_2MoCl_2 with HSA in $tris_d$ buffer at physiological pH at a temperature of 25°C.

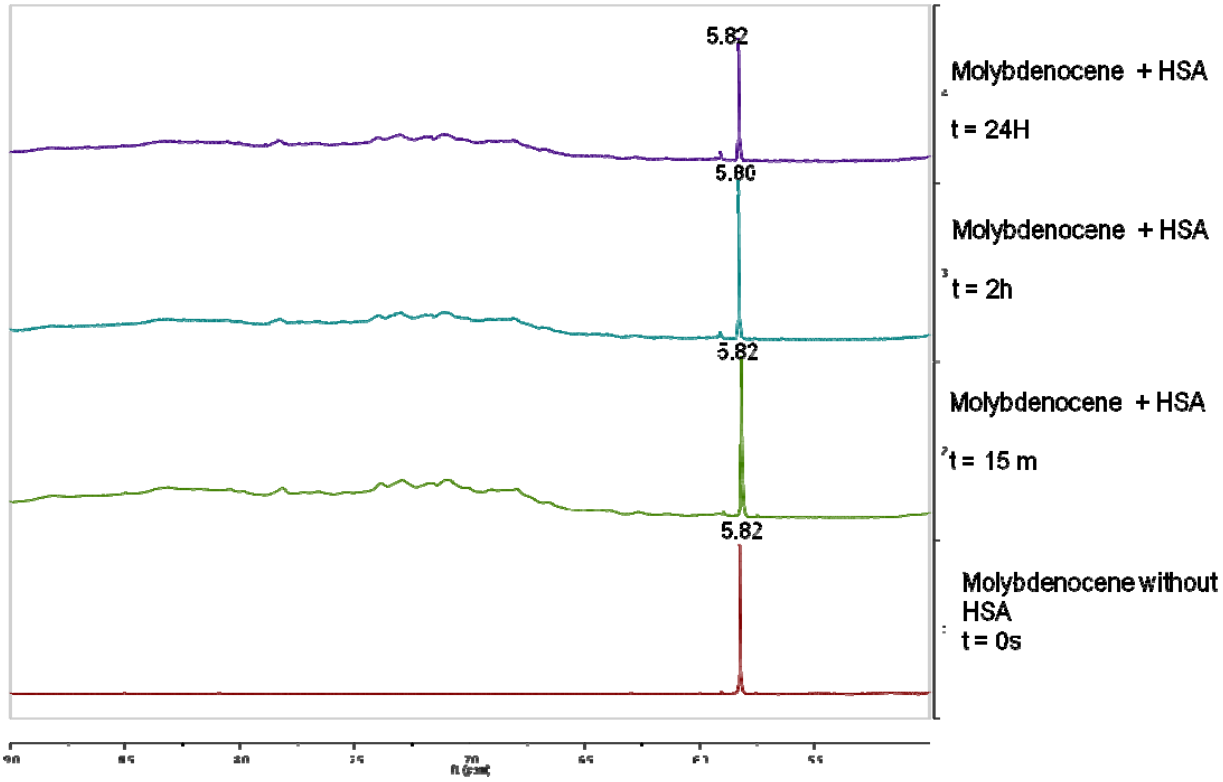

Figure 28 **T**he 500MHz ^{1}H NMR spectra at different time intervals of the interaction of Cp_2MoCl_2 with HSA in $tris_d$ buffer at physiological pH at a temperature of 37°C.

3.4 Cytotoxic Studies

3.4.1 HT-29 Cell line

Biological activity for molybdenocene dichloride and its derivatives was determined with MTT assay. The assay was done on the human colon cancer cell line HT-29 for a period of 72 hours with complex concentrations from approximately 0.01 to 0.00001 M. In order to find the concentration of the complex that is required to inhibit 50% of the cell growth, a dose-response curve was constructed. This curve consists on plotting response vs. concentration of the complex or drug (agonist) which exhibits a sigmoidal shape. This plot is also known as a standard dose-response curve which is defined by the percent of viability (bottom) and the drug concentration that induces changes in the cell viability. The 50% inhibition concentration, also known as IC_{50}, can be obtained from the described plot by using Prism software [48]. This quantity indicates how much of a particular drug is needed to inhibit a given biological process by 50%.

The IC_{50} values against HT-29 obtained for the $[Cp_2Mo(6\text{-mercaptopurine})]Cl$, $[Cp_2Mo(6\text{-mercaptopurine ribose})]Cl$, $[Cp_2Mo((-)\text{-2-amino-6-mercaptopurine})]Cl$ and $[Cp_2Mo((-)\text{-2-amino-6-mercaptopurine ribose})]Cl$ complexes were 0.180(±0.008) mM, 0.201(±0.045) mM, 0.015(±0.016) mM and 0.277(±.025) mM, respectively. These studies suggest that drug effectiveness decreases in the following complex order: $[Cp_2Mo((-)\text{-2-amino-6-mercaptopurine})]Cl > [Cp_2Mo(6\text{-mercaptopurine})]Cl > [Cp_2Mo(6\text{-mercaptopurine ribose})]Cl > [Cp_2Mo((-)\text{-2-amino-6-mercaptopurine ribose})]Cl$. Among the four complex under study, $[Cp_2Mo((-)\text{-2-amino-6-mercaptopurine})]Cl$ proved to be approximately ca. 10 times more cytotoxic than the other three complexes, within the experimental error.

Previous studies of IC_{50} values against HT-29 obtained for Cp_2MoCl_2 showed that the required concentration to inhibit 50% of cells proliferation was 2.6(±0.3) mM. This suggests

that molybdenocene derivatives presented in this work are more effective against HT-29. The replacement of the two chlorides in Cp_2MoCl_2 by thionucleobase/thionucleoside ligands improves the cytotoxic activity of molybdenocene.

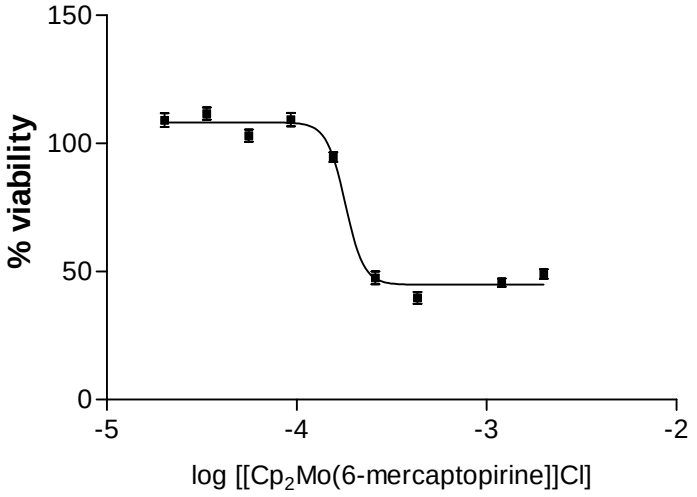

Figure 29 **D**ose-response curves for [Cp2Mo(6-Mercaptopurine)]Cl against HT-29 cell at drug exposure of 72 hours.

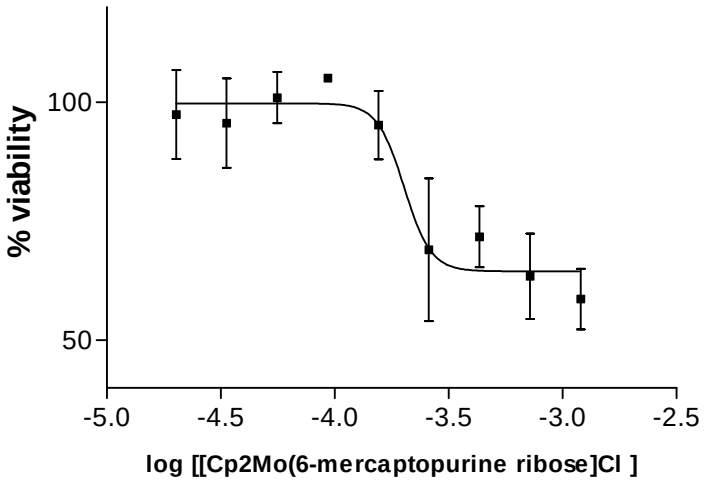

Figure 30 Dose-response curves for [Cp2Mo(6-Mercaptopurine ribose)]Cl against HT-29 cell at drug exposure of 72 hours.

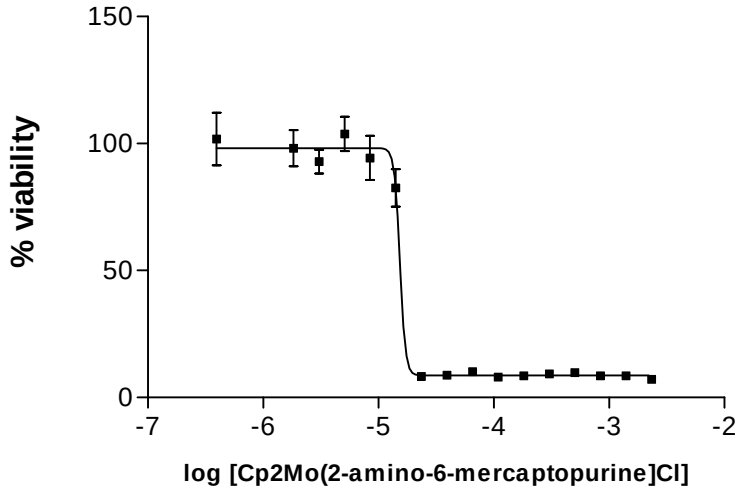

Figure 31 Dose-response curves for [Cp2Mo((-)-2-amino-6-Mercaptopurine)]Cl against HT-29 cell at drug exposure of 72 hours.

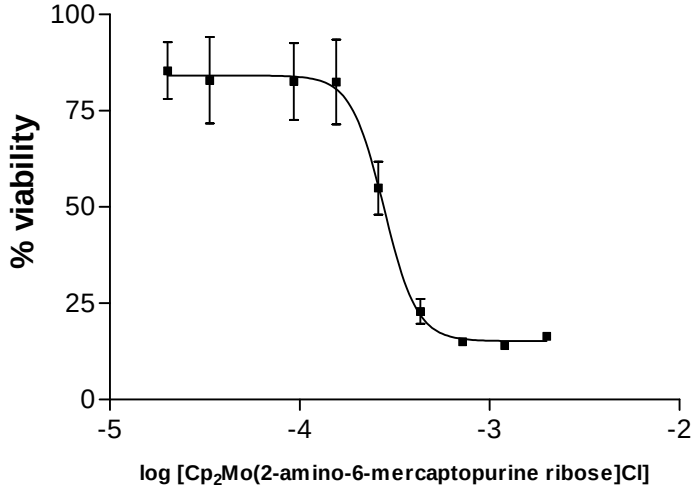

Figure 32 Dose-response curves for [Cp2Mo((-)-2-amino-6-Mercaptopurine ribose)]Cl against HT-29 cell at drug exposure of 72 hours.

3.4.2 MCF-7

The IC_{50} values for MCF-7 were obtained following the same procedure as for HT-29. The IC_{50} against MCF-7 obtained for the [Cp_2Mo(6-mercaptopurine)]Cl, [Cp_2Mo((-)2-amino-6-mercaptopurine)]Cl complexes were 0.203(±0.045) mM and 0.016(±0.002) mM, respectively. The complexes [Cp_2Mo(6-mercaptopurine ribose)]Cl and [Cp_2Mo(2-amino-6-mercaptopurine ribose)]Cl resulted to be not active.

The cytotoxic activity of Cp_2MoCl_2 in MCF-7 cell line has been studied [32]. In contrast to HT-29 a proliferative behavior was reported for the complex Cp_2MoCl_2 in MCF-7 cell line [32]. Taking this into account it can be said that in MCF-7, the addition of a thionucleoside does not contribute to the cytotoxic activity of molybdenocene. Meanwhile, the addition of a thionucleobase enhances the cytotoxic activity of molybdenocene.

Contrary to the results obtained for the dose-response of the HT-29 cell line, in the MCF-7 cell line the complex Cp_2MoCl_2 exhibits proliferative behavior while the complexes [Cp_2Mo(6-mercaptopurine ribose)]Cl and [Cp_2Mo((-)2-amino-6-mercaptopurine ribose)]Cl resulted to be not active. It should be pointed out that 6-mercaptopurine and its derivatives have cytotoxic activity several cancer cell lines including colon in the milimolar range. [42-44] Therefore, the enhancement in cytotoxic activity of molybdenocenes with mercaptopurines in HT-29 colon cancer cell line could be the result of the thionucleobases activities.

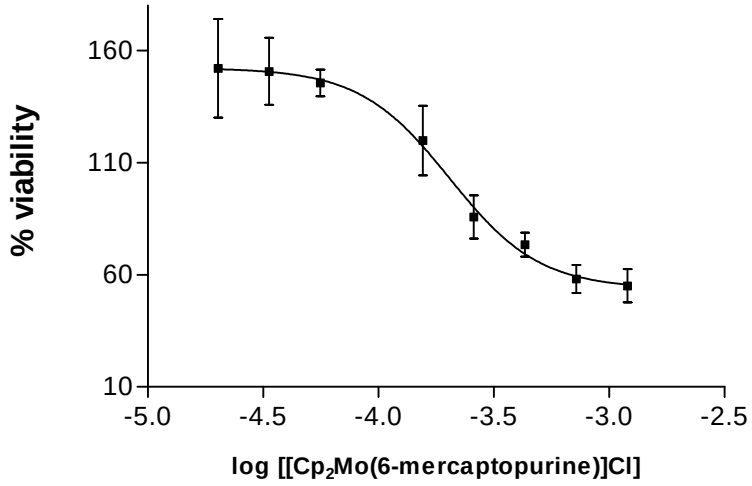

Figure 33 Dose-response curves for [Cp2Mo(6-Mercaptopurine)]Cl against MCF-7 cell at drug exposure of 72 hours.

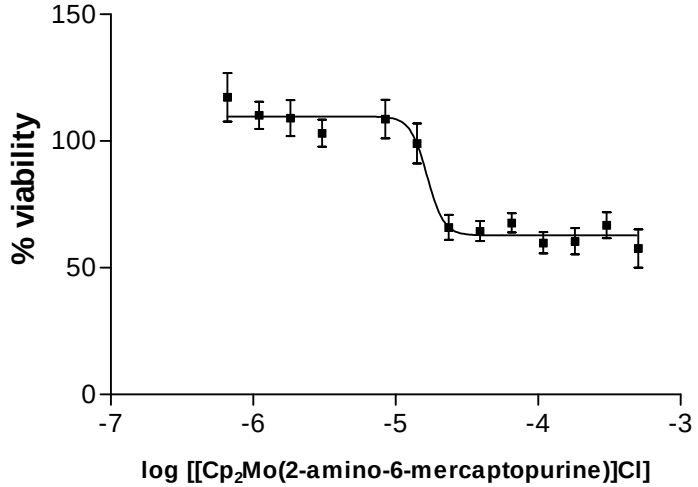

Figure 34 Dose-response curves for [Cp2Mo((-)-2-amino-6-Mercaptopurine)]Cl against MCF-7 cell at drug exposure of 72 hours.

4. Conclusion and Future Work

A new methodology has been developed for molybdenocene derivatives containing thionucleobases or thionucleoside judged by spectroscopic and spectrometric methods. These reactions can be carried out at physiological pH aqueous medium which enhance the reported reactions in a tetrahydrofuran/methanol solvent mixture. This characteristic makes these complexes more prominent since it makes them closer to possible chemotherapeutics.

Citotoxicity studies suggest that the four new molybdenocene derivatives improve the citotoxicity activity toward the HT-29 colon cancer when compared to molybdenocene dichloride. Within these complexes those that contained ribose showed to be less active than those without ribose but all complexes proved to have more activity than molybdenocene dichloride in the citotoxicity activity toward HT-29 colon cancer. The ribose group might add bulkiness to the complex thus making it less effective in cell activity. From the two more active complexes it can be inferred that the amino group enhances the activity in the cell. This makes this type of drug more active at less concentration. In MCF-7 breast cancer the addition of these bidentate ligands without a ribose group, improves the cytotoxic activity when compared to Cp_2MoCl_2. On the other hand the complex with the ribose group showed to be not active in MCF-7 cell line. This lack of activity has also been attributed to the bulkiness of the complex due to the ribose.

Substituting chloride by thionucleobases/thionucleoside does not enhance the molybdenocene capacity to bind human serum albumin. It has been observed that vanadocene dichloride has demonstrated to be a very active complex in colon cancer cell line and it interacts with transferrin [26, 32, 38]. These facts could contribute to future works where synthesis and

characterization of vanadocene complexes with thionucleobases/thionucleoside can be done. These complexes can validate if thionucleobases/thionucleoside ligands enhance the citotoxic capacity of vanadocene and in their interaction with apotranferrin.

5. References

1. National Cancer Institute http://www.cancer.gov/cancertopics/cancerlibrary/what-is-cancer (accessed march 2010)
2. Reedijk, J.; *PNAS* (2003), 100(7), 3611-3616
3. Rosenberg, B.; Van Camp, L.; Krigas, T.; *Nature* **(1965)**, *205*, 698–699.
4. Sadler, P.J.; Guo, Z.; *Pure & Appl. Chem.* **(1998)**, 70(4), 863-871
5. Rosenberg, B.; Van Camp, L.; Trosko, J. E.; Mansour, V. H.; *Nature* **(1969)** , *222*, 385–387.
6. Abrams, M.J.; Murrer, B.A.; *Science*, **(1993)** , 261, 725-730
7. Kopf, H.; Kopf-Maier, P.; *Angew. Chem. Int. Ed. Engl.* **(1979)** ,18, 477
8. Manohari Abesysinghe, P.; Harding, M. M.; *Dalton Trans.* **(2007)**, 3474-3482
9. Kopf-Maier, P; Kopf, H.; *Chem. Rev.* **(1987)**, 87, 1137
10. Kopf-Maier, P; Kopf, H.; *J. Organomet. Chem*. **(1988)**, 342, 167.
11. Harding, M.M.; Mokdsi, G.; *Curr. Med. Chem*. **(2000),** 7, 1289-1303.
12. Guo, M.; Sun, H.; McArdle, H.J.; Sadler, P.J.; *Biochemistry* **(2000),** 93, 10023
13. Melendez, E.; *Crit. Rev. Oncol. Hematol.* **(2002)**, 42, 309.
14. Kopf, H.; Kopf-Maier, P.; *Inorg. Chim. Acta* **(1985)**, 108, 99-103
15. Ghosh, P.; O.J.D. Cruz; Narla R. K.; and Uckun F.M.; *Clinical Cancer Research* **(2000)** 6, 1536-1545.
16. Toney J.H.; Marks T. J.; *J. Am. Chem. Soc.* **(1985)** 107, 947
17. Kuo L. Y.; Kanatzidis M. J.; Marks T. J.; *J. Am. Chem. Soc.* **(1987),** 109, 7207.
18. Vinklarek, J.; Honzicek, J.; Holubová, J.; *Inorg. Chim. Acta* **(2004),** 357, 3765-3769
19. Pérez, Y.; López, V.; Rivera-Rivera, L.; Cardona, A.; *J Biol Inorg Chem* **(2005)** 10, 94–104

20. Erxleben, A.; Kottmann, J.; *Inorg. Chimica Acta* **(2006)**, 359, 13–24

21. Palackova, H.; Vinklarek, J.; Holobová, J.; Cisarova, I.; Erben, M.; *J. Organomet. Chem*. **(2007)**, 692, 3758–3764

22. Sun, H.; Cox, M. C.; Li, H.; Mason a. B.; Woodworth, R. C.; Sadler, P.J.; *FEBS Letters.* **(1998),** 422, 315-320.

23. Li, H.; Sadler P. J.; Sun H.; *JBC* **(1996)**, 271 9483-9489.

24. Cardona A.; Meléndez E.; *Anal. Bioanal. Chem.* **(2006)**, 386, 1689–1693

25. Gunter Grossmann, J.; Neu, N.; Evans, R. W.; Lindley, P. F.; Appel, H.; Samar Hasnain, S.; *J. Mol. Biol.* **(1993),** 229, 585-590

26. Nishida Y.; Niiunuma, A.; Abe, K.; *Inor. Chem. Comm.* **(2009)**, 12, 198-200

27. Campbell, K. S.; Dillon, C. T.; Smith, S. V.; Harding, M. M.; *Polyhedron* **(2007)**, 26(2), 456-459

28. Tinoco, A.D.; Incarvito, C.D.; Valentine, A.M.; *J. Am. Chem. Soc.* **(2007),** 129, 3444 – 3454

29. Tinoco, A. D.; Eames, E. V.; Valentine, A. M.; *J. Am. Chem. Soc.* **(2008),** 130, 2262-2270

30. Gao, L; Hernandez, R.; Matta, J.; Melendez, E.; *J. Biol. Inorg.Chem.* **(2007),** 12, 959-967.

31. Hernandez, R.; Lamboy, J.; Gao, L; Matta, J.; Roman, F. R.; Melendez, E.;. *J. Biol. Inorg. Chem.* **(2008)**, 13, 685-692.

32. Feliciano, I.; Matta, J.; Melendez, E.; *J. Biol. Inorg. Chem.* **(2009),** 14**,** 1109-1117

33. Vera, J.L.; Roman, F.; Melendez, E.; *Anal.Bioanal. Chem.* **(2004),** 379, 399-403.

34. Rodriguez, M.I.; Chavez-Gil, T.; Colon, Y.; Diaz, N.; Melendez, E.; *J. Electroanal. Chem.* **(2005)**606 576:315

35. Melendez, E.; Marrero, M.; Rivera, C.; Hernandez, E.; Segal, A.; *Inorg. Chim. Acta* **(2000)** 298, 178-186

36. Bariyanga, J.; Luyt, A. S.; *J. Mol. Structure* **(2001),** 559, 49-54

37. Chavez-Gil, T. E.; Melendez, E.; *Inorg. Chim. Acta* **(2004),** 357, 1092-1102

38. Cardona-Mejias, A. Thesis, University of Puerto Rico, **(2006).**

39. Garcia Tasende, M. S.; Suarez Gimeno, M.I.; Sanchez, A.; Casa, J.S.; *J Organ. Chem.* **(1990)**, 384, 19-24

40. Hernandez-Castillo, R. L. Thesis, University of Puerto Rico, **(2008).**

41. Feliciano-Caraballo, I.; Thesis, University of Puerto Rico **(2009).**

42. Temple, C. Jr.; Kussner, C. L.; Montgomery, A.; *J. Med. Chem.* **(1968), 11, 41-44**

43. Calatayud, S.; Warner, T. D.; Mitchell, J. A. *Br J Cancer*. **(2002),** 8, 163-167

44. Gunnarsdottir, S.; Elfarra, A.; *Drug Metab. Dispos.* **(2004),** 32, 321-327

45. Kuo, L. Y.; Kanatzidis, M.; Sabat, M.; Tipton, A. L.; Marks, T. J.; *J. Am. Chem. Soc*. **(1991)**, 92, 9027

46. Sugio, A.; Kashima, A.; Mochizuki, S.; Noda, M.; Kobayashi, K.; *Protein Eng.* **(1999)**, 12, 439-446

47. He, X. M.; Carter, D. C.; *Nature* **(1992),** 358, 209-215

48. GraphPad Prism Version 3.02, April 25, 2000
Copyright 1994-2000
GraphPad Software incorporated